# Fabrication and utilization of bifunctional protein/polysaccharide coprecipitates for the independent codelivery of two model actives from simple oil-in-water emulsions

Spyropoulos, Fotis; Kurukji, Daniel; Taylor, Phil; Norton, Ian T

*DOI:*
10.1021/acs.langmuir.7b04315



*Document Version*
Peer reviewed version

*Citation for published version (Harvard):*
Spyropoulos, F, Kurukji, D, Taylor, P & Norton, IT 2018, 'Fabrication and utilization of bifunctional protein/polysaccharide coprecipitates for the independent codelivery of two model actives from simple oil-in-water emulsions', *Langmuir*, vol. 34, no. 13, pp. 3934–3948. https://doi.org/10.1021/acs.langmuir.7b04315

# Fabrication and utilisation of bi-functional protein/polysaccharide co-precipitates for the independent co-delivery of two model actives from simple oil-in-water emulsions

*Fotis Spyropoulos[1*], Daniel Kurukji[1], Phil Taylor[2], Ian. T. Norton[1]*

[1]School of Chemical Engineering, University of Birmingham, UK
[2]Formulation Technology Group, Syngenta Ltd, Jealott's Hill International Research Centre, UK

**KEYWORDS.** *Protein/polysaccharide complexation; Pickering emulsions; co-encapsulation; co-delivery; sustained release; triggered release*.

## ABSTRACT

Aside from single active microencapsulation, there is growing interest in designing structures for the co-encapsulation and co-delivery of multiple species. Although currently achievable within solid systems, significant challenges exist in realising such functionality in liquid formulations. The present study reports on a novel microstructural strategy that enables the co-encapsulation and co-release of two actives from oil-in-water emulsions. This is realised through the fabrication of sodium caseinate/chitosan (NaCAS/CS) complexes that in tandem function as encapsulants of one active (hydrophilic) but also as ('Pickering-like') stabilisers to emulsion droplets containing a secondary active (hydrophobic). Confocal microscopy confirmed that the two co-encapsulated actives occupied distinct emulsion microstructure regions; the hydrophilic active was associated with the NaCAS/CS complexes at the emulsion interface, while the hydrophobic active was present within the oil droplets. Aided by their segregated co-encapsulation, the two actives exhibited markedly different co-release behaviours. The hydrophilic active exhibited triggered-release that was promoted by changes to pH, which weakened the protein-polysaccharide electrostatic interactions resulting in particle swelling. The hydrophobic secondary active exhibited sustained release that was impervious to pH and instead controlled by passage across the interfacial barrier. The employed microstructural approach can therefore lead to the segregated co-encapsulation and independent co-release of two incompatible actives, thus offering promise for the development of liquid emulsion-based formulations containing multiple actives.

## Introduction

The development of technological approaches enabling the encapsulation and delivery of functional species (e.g. active ingredients) is an area of major academic and industrial research activity with relevance to a wide range of applications (e.g. food, pharmaceutical, agrochemical).[1]-[3] Aside from typical microencapsulation, which focuses on the encapsulation and controlled/triggered delivery of a single active, there is also growing interest in designing structures that enable the co-encapsulation and co-delivery of two or more functional molecules within/from a sole formulation.[4]-[6] The pharmaceutical industry has been at the forefront of research activity in this area in order to develop pharmaceutical combination therapies, and in particular fixed-dose combination medicines, where the co-delivery of multiple active pharmaceutical ingredients (APIs) from a single formulation is required.[6],[7] Although this has been indeed realised for solid dosage forms through the utilisation of various processing approaches including 3D-printing,[8] co-delivery from liquid formulations, which amongst others offer dosage flexibility and addresses dosage form needs of specific patient populations (e.g. paediatrics, geriatrics), is limited.[5],[9]

Emulsions are attractive microstructures for the encapsulation and delivery of functional molecules within/from liquid formulations.[10],[11] This is due to their multiphase attributes, ease of formation, as well as their utilisation in a number of structured liquid/semi-liquid products.[12] Despite this, present encapsulation and delivery approaches within emulsions are usually only concerned with the encasing and release of a single active ingredient. More complex emulsion/colloidal architectures, such as microemulsions,[13] double emulsions[5],[14],[15], polysaccharide-based nanocomplexes[16], liposomes[17],[18] and niosomes[19], have been put forward as potential candidates designed for the co-encapsulation/co-release of incompatible actives within/from a liquid disperse phase system. However, these types of structures have been associated with major stability issues and in some cases their large-scale manufacturing would require a significant level of interference to current technical/processing industrial infrastructure.[14],[18],[20],[21] In addition, the co-delivery performance of these microstructures is limited to simultaneous or sequential rather than independent release profiles; i.e. the release of one active is directly linked to that of the other (active) species and as such cannot be separately triggered/controlled.[16],[17]

In terms of applications, simple oil-in-water (o/w) or water-in-oil (w/o) emulsions designed to enable the co-encapsulation of multiple actives in a segregated manner could prove useful for the co-delivery of incompatible (including components of markedly different hydrophilic/hydrophobic characteristics) or chemically reactive species.[22],[23] Such a co-encapsulation/co-delivery approach would also be useful when co-release (from within the same liquid formulation) is required over different timescales and/or in response to external and potentially disparate stimuli/triggers (e.g. pH, magnetic field, mechanical stress).[22],[24] Opportunities for co-encapsulation/co-delivery liquid formulations also exist within the next-generation biomedical/pharmaceutical, agrochemical, functional food, paint, and adhesive arenas.[13],[25],[26] However, it should be recognised that such delivery systems are still in their

infancy and thus fundamental and translational research efforts are required to develop such concepts further.

Pickering emulsions differ from conventional emulsions in that particulate species rather than surfactants or polymeric components are employed to stabilise the liquid-liquid interface against coalescence and/or other destabilisation phenomena.[27],[28] Chemistries historically investigated for use in Pickering particle fabrication primarily include inorganic materials such as clays and silicas.[29],[30] However, in recent years, focus has shifted towards natural materials (e.g. proteins, polysaccharides, lipids)[31],[32] in response to drivers from the food and pharmaceutical sectors, which would require such Pickering structures to be fabricated from a relatively limited number of approved building blocks.[33] The design of novel anisotropic particles (e.g. Janus particles),[34]-[36] which are characterised by their well-defined, dual- or multi-hemisphere surface chemistry has fed into Pickering stabilisation as one possible area of application for surface active and amphiphilic particles. However, key challenges remain in developing scalable processes for the production of anisotropic particles,[21],[37] proposing valued-added applications and lastly, utilising renewable, bio-based ingredients for their manufacture. When carefully designed and fabricated, solid particles employed as Pickering stabilisers confer well-defined functional attributes upon the resulting emulsion;[38]-[40] these include 'programmable' instability and modulated/triggered encapsulation/delivery behaviours.[10],[11],[24],[41],[42] In turn, this can translate into a number of exciting and value-added opportunities in encapsulation and molecular delivery, including the development of liquid pharmaceutical dosage forms designed to target different parts of the digestive tract.[43]

The functional particles utilised in the present study have been fabricated from common biopolymers; sodium caseinate (protein) and chitosan (polysaccharide). These biopolymers are frequently employed, and cited for use, in food and pharmaceutical applications.[44],[45] Formation of the biopolymer assembly in this instance capitalises on the concept of electrostatic complexation, which is promoted by a controlled pH environment that renders the two polymeric species to become oppositely charged.[46]-[50] The capacity of protein/polysaccharide complexes to stabilise emulsions (and foams) has been extensively reported[51],[52], with literature in the area predominantly focusing either on protein/polysaccharide conjugates[53] or protein/polysaccharide (complex) coacervates[54]. Although stabilisation is provided by the adsorption of protein/polysaccharide complexes (in many cases) as intact entities at the emulsion interface, these systems have been historically differentiated from classical solid Pickering particles. Nonetheless, recent studies have drawn direct parallels between these two distinct classes of colloidal structures in terms of their capacity to stabilise emulsions, suggesting that even electrostatic protein/polysaccharide complexes can exhibit Pickering-like interfacial functionality.[55],[56] Previous work[48] has reported on the fabrication of the sodium caseinate/chitosan colloidal complexes utilised in the current study, on the formulation and processing elements that impact upon their size and stability, and finally on their encapsulation efficiency and capacity to provide pH-triggered delivery of model hydrophilic active compounds; fluorescein and rhodamine B. This earlier work[48] however did not assess the Pickering functionality of the sodium caseinate/chitosan

colloidal assemblies and only focused on their ability to act as vehicles for the encapsulation and triggered release of model hydrophilic actives.

The present work aims to study the capacity of sodium caseinate/chitosan complexes to stabilise simple o/w emulsions in order to demonstrate whether these biopolymer architectures can be utilised as bi-functional Pickering particles; i.e. as structures that can in tandem act as encapsulation vehicles for the targeted delivery of an active as well as Pickering particles providing emulsion stabilisation in the absence of additional surfactant/emulsifier species. The current study then progresses further to investigate whether these bi-functional Pickering particles can facilitate the segregated co-encapsulation and independent co-delivery, within/from simple oil-in-water emulsions, of two incompatible model actives (one hydrophilic active associated with the biopolymer complexes and another hydrophobic active placed within the oil core of the emulsion droplets), thus enabling the development of novel emulsion-based liquid formulations containing multiple actives.

## 2. Experimental Section

### 2.1 Materials

Sodium caseinate (NaCAS) from bovine milk (CAS number: 9005-46-3), low molecular weight (MW: 50-190 kDa) chitosan (CS) with a de-acetylation degree of 75-85% (CAS number: 9012-76-4) rhodamine B (RhodB), fluorescein sodium salt (FSS), dimethylphthalate (DMP), perylene (PE), sodium azide ($NaN_3$) and acetic acid (≥99.7% purity), were all obtained from Sigma-Aldrich (UK) and used without further purification. RhodB or FSS, used as model Active 1 (hydrophilic), were encapsulated within the sodium caseinate/chitosan (NaCAS/CS) complexes. DMP or PE were employed as model Active 2 (hydrophobic), the former for release experiments while the latter for confocal microstructure visualisation purposes only. The oil phase used in all cases for emulsion preparations was commercially available sunflower oil. Water used throughout this study was passed through a double-distillation column equipped with a de-ionisation unit. Concentrations of all material are given as percentages of the weight of the specific substance over the total weight of the system it is contained within (i.e. dispersion, emulsion, etc.) and are denoted as ‘wt.%’.

### 2.2 Methods

#### *2.2.1 Particle preparation*

Aqueous suspensions of the NaCAS/CS complexes were prepared in a sodium acetate aqueous buffer (30 mM) at pH 5. Unless otherwise stated in the manuscript, biopolymer complexes were fabricated at a fixed total biopolymer concentration (TBC) of 1 wt.% and for chitosan-to-sodium caseinate mass ratios of 1/3, 1/1, and 3/1; as such complexes with CS mass fractions of 0.25, 0.5 and 0.75, respectively, were produced. In those cases were encapsulation of Active 1 was studied, the biopolymer assemblies were formed in the presence of a fixed mass of RhodB or FSS. Stock

solutions of RhodB or FSS (in buffer at pH 5) were prepared at 0.007 mg $g^{-1}$ (for RhodB) or 0.2 mg $g^{-1}$ (for FSS) of sodium acetate aqueous buffer (30 mM). 5.5 g of stock solution was then added to 50 g of the appropriate mixed biopolymer solution and production of the suspended NaCAS/CS complexes then followed. The final RhodB and FSS loading in the resulting systems, unless otherwise stated, was therefore approximately 0.7 µg $g^{-1}$ and 20 µg $g^{-1}$ of aqueous suspension, respectively. A small quantity of sodium azide (0.03 wt.%) was added to all systems in order to limit/arrest microbial degradation during storage. It should be noted that in both cases the final loadings for the two components were significantly lower than their aqueous solubilities; 10 mg $g^{-1}$ for RhodB[57] and 500 mg $g^{-1}$ for FSS (Sigma-Aldrich), respectively. In order to reduce the size of the initially formed complexes (typically of the order of several hundred micrometres)[48], all aqueous suspensions were subjected to ultrasonic processing (Viber Cell 750, Sonics, USA) using a 12 mm diameter probe for 2 min (20 kHz, 95% amplitude). A more detailed description on the fabrication of the NaCAS/CS complexes and the encapsulation of Active 1 within these is given in a previous study by the authors.[48]

### *2.2.2 Particle size analysis*

Following sonication, the z-average particle diameters of the resulting colloidal NaCAS/CS complexes were measured by dynamic light scattering (DLS) using a Zetasizer (Nano ZS) Nano Series (Malvern, UK). Typically, two drops from the formed (at pH 5) aqueous suspension of NaCAS/CS complexes were added (diluted) into 25 g of sodium acetate aqueous buffer (also at pH 5) and then immediately transferred to a polystyrene cuvette for DLS measurement. In addition, NaCAS/CS complexes (formed at pH 5) were exposed to a range of pH conditions and their z-average particle diameters (following pH adjustment) were measured similarly to above; however in this case dilution was carried out in buffer solutions of the same pH value as that in the pH-adjusted colloidal suspension.

### *2.2.3 Zeta potential*

Zeta-potential analyses were performed on a Zetasizer (Nano ZS) Nano Series equipped with an MPT-2 multipurpose titrator (Malvern, UK). For zeta-potential measurements of NaCAS/CS complexes fabricated at varying CS mass fractions, the aqueous suspensions were diluted as for particle size analyses and added to a specialised zeta cell (Malvern, UK).

### *2.2.4 Surface Tension*

Surface tension measurements were carried out at 20°C using the Wilhelmy plate method on a K100 Tensiometer by Krüss GmbH (Germany). Evaporation was controlled using a plastic cover inserted over the sample.

### *2.2.5 Emulsion preparation*

The produced suspensions of NaCAS/CS complexes (of different chitosan mass fractions) were used as the aqueous phase for the preparation of all emulsions. The oil phase used for emulsion

production comprised a blend of sunflower oil (SFO) and DMP or PE, both prepared by mild mixing on a magnetic stirrer. For emulsion droplets containing DMP, the oil phase comprised DMP and SFO at a fixed mass ratio of 6/56 (DMP/SFO), while for those including PE, the oil phase contained 20 mg of PE per litre of SFO. In either case, 10 g of the oil phase containing Active 2 (DMP or PE) was added to 40 g of the aqueous phase (aqueous suspensions of NaCAS/CS complexes) containing Active 1 (for emulsion preparations only RhodB was used as model Active 1) at each chitosan mass fraction and emulsified for 5 minutes at 8000 rpm using a Silverson High Shear Mixer fitted with an Emulsor Screen of medium (standard) perforations. Sample temperature was not controlled during high shear mixing and this was found to increase to no more than 10°C above room temperature (also the initial temperature of the system prior to emulsification). A small quantity of sodium azide (0.03 wt.%) was added to all emulsions in order to limit/arrest microbial degradation during storage. All prepared o/w emulsions were therefore at a fixed oil-to-water mass fraction of 20/80 (wt.%/wt.%).

### *2.2.6 Emulsion droplet size analysis*

Droplet size distributions of the formed o/w emulsions were measured by laser diffraction using a Malvern Mastersizer 2000S (Malvern Instruments, UK) equipped with a Hydro S dispersion cell. Emulsions were quiescently stored at 40°C and were assessed in terms of their stability against coalescence over a two-month storage period, by monitoring changes to their average droplet diameters (expressed throughout this study as the surface weighted mean diameter, $D_{3,2}$).

### *2.2.7 Microscopy*

Selected aqueous suspensions of NaCAS/CS complexes and o/w emulsions were visualised using light microscopy; typically, a single drop from the suspension or emulsion was placed on a glass slide with a cover slip and then analysed/visualised. In addition, confocal microscopy was used to confirm the positioning of the co-encapsulated actives within the emulsion microstructure. An emulsion, with PE (Active 2) encapsulated within its droplets and stabilised by NaCAS/CS complexes (TBC of 1 wt.% and CS mass fraction of 0.25) also containing RhodB (Active 1), was analysed using a Leica TCS SPE (Leica, Germany) confocal microscope. The emulsion was diluted ten times in sodium acetate buffer (30 mM, pH 5). A drop from this emulsion was placed on a glass microscope slide and a cover slip was glued on top to fix it in place. Separate fluorescent emission spectra were obtained for RhodB and PE, enabling spatial identification of each active within the emulsion microstructure.

### *2.2.8 Fractional Encapsulation Efficiency (FEE)*

Fractional Encapsulation Efficiency (FEE) of Active 1 (RhodB or FSS) within the formed complexes was determined by transferring 1.5 mL of the aqueous suspension of complexes (before and after sonication) to separate Eppendorf tubes and centrifuging (Sigma 3k30, SciQuip, UK) for 60 minutes at 15,000 rpm. The centrifugation time used had been previously determined in a separate series of preliminary experiments as sufficient in order to separate the NaCAS/CS

complexes as an insoluble pellet at the bottom of the Eppendorf tube. The supernatant was analysed by ultraviolet-visible (UV-VIS) spectroscopy (Libra S12, Biochrom, UK) at the following wavelengths for each active: RhodB at 550 nm and FSS at 460 nm. Using Beer's law the mass of active (Active 1) in the supernatant ($M_0^{sup}$) was calculated over its linear range using a previously determined calibration curve. FEE was then calculated using:

$$\text{FEE} = \frac{M_{\max} - M_0^{\sup}}{M_{\max}} \qquad \text{Eq. 1}$$

where $M_{max}$ is the total mass of active that was initially introduced into the system.

DMP was used as the model Active 2 in order to monitor release from within the formed emulsion oil droplets. DMP was selected as a model active as it is soluble in the oil phase while at the same time it has an appreciable water solubility (4 mg $g^{-1}$)[58]. As previously described, DMP is introduced as a blend with SFO and the mixture is then dispersed in an aqueous phase to form the o/w emulsions. DMP has a reported[58] octanol-water partition coefficient of 33, which means that for an o/w emulsion with a 20% oil mass fraction, the highest percentage of total DMP residing within the aqueous continuous phase is not expected to exceed a value of approximately 10%; this value is expected to slightly vary for SFO (compared to octanol). Even in the absence of SFO-water partition coefficient data, it is still anticipated that DMP will primarily remain within the oil phase and as such for the purpose of this study it is assumed that upon emulsion preparation the Fractional Encapsulation Efficiency (FEE) of DMP within the formed oil droplets is equal to 1.

### *2.2.9 Release measurements*

*Release from NaCAS/CS complexes*. Release of Active 1 (RhodB or FSS) from the formed NaCAS/CS complexes was monitored as a function of pH with a glass pH probe and SevenEasy meter (Mettler Toledo, Switzerland) at a fixed TBC of 1 wt.% and a CS mass fraction of 0.25. In a typical release experiment, 55.5 g of an aqueous NaCAS/CS suspension, formed at pH 5 and also containing FSS, were placed in a beaker and mildly stirred on a magnetic plate. Small aliquots (50-1000 μL) of a 10% NaOH solution were added to increase the suspension's pH in small intervals from pH 5 to approximately pH 11; in total, addition of approximately 2-3 mL of the NaOH solution were required for pH adjustment. When each pH interval had been reached, a 1.5 mL aliquot was withdrawn from the suspension and transferred to an Eppendorf tube. These withdrawn samples were centrifuged (Sigma 3k30, SciQuip, UK) at 15,000 for 60 min and the concentration of FSS in the supernatant was determined following the same procedure described earlier for FEE determination. FSS has an isosbestic point at 460 nm, which enabled its concentration to be obtained independent of the pH change. However, due to its acid-base chemistry it was not possible to quantify FSS concentration at low pH values (i.e <pH 5). Instead, RhodB was preferentially used to monitor entrapment/release at conditions below pH 5. For RhodB, the active-containing NaCAS/CS complex suspension was firstly titrated down to pH 2 by addition of small aliquots (50-1000 μL) of a 10% HCl solution. Subsequently, pH was increased to pH 11 (similarly to FSS-containing systems) and 1.5 mL samples were taken at desired pH intervals as described above for

FSS. RhodB did not exhibit a pH dependent absorbance at the wavelength employed for analysis in the UV-VIS spectrophotometer (550 nm). The concentrations for RhodB or FSS (both representing Active 1) in the release studies were significantly lower than their solubilities in the aqueous acceptor phase (see previous section) and therefore it is assumed that release of Active 1 from the formed NaCAS/CS complexes is taking place under sink conditions.

*Co-Release from o/w emulsions*. Measurements of the co-release of Active 1 (only RhodB was employed in the co-release studies) and Active 2 (DMP) were carried out for an emulsion system stabilised by biopolymer complexes with a fixed TBC of 1 wt.% and a CS mass fraction of 0.25. Within the produced emulsion microstructure, Active 1 (RhodB) and Active 2 (DMP) were co-encapsulated within the biopolymer complexes and dispersed phase droplets, respectively. In a typical experiment, 20 g of the emulsion were placed within a semi-permeable cellulose dialysis membrane (ca. 20 mm x 150 mm), which had previously been soaked in water for 24 h. The molecular weight cut-off and surface area of the membrane were kept constant such that any effects from these parameters were normalised. This emulsion-containing membrane was then submersed in 1000 g of sodium acetate buffer (30 mM, pH 5) inside a conical flask, which was mildly stirred throughout the experimental time frame to facilitate exchange of material between the contents of the dialysis tubing and the acceptor phase. 3 mL aliquots of the external aqueous acceptor phase were periodically collected over a period of 48 hours. The ultraviolet-visible (UV-VIS) absorbance (Libra S12, Biochrom, UK) of these samples was measured at active-specific wavelengths (550 nm for RhodB and 280 nm for DMP, respectively) in a quartz cuvette. Using predetermined linear calibration curves, the mass of Active 1 (RhodB) and Active 2 (DMP) present in the acceptor phase were determined. In order to investigate release kinetics as a result of changes to the system's pH environment, the starting pH of the acceptor phase was altered outside of the buffer region (originally at pH 5) to pH 3 or pH 10 using solutions of hydrochloric acid or sodium hydroxide, respectively, as appropriate.

Assuming that both actives eventually fully migrate across the dialysis membrane, their final concentrations in the aqueous acceptor phase will be approximately 0.01 μg $g^{-1}$ for RhodB and 0.39 mg $g^{-1}$ for DMP, respectively. As these concentrations are both significantly lower than the individual solubilities for the two species, co-release of Active 1 (RhodB) and Active 2 (DMP) is expected to take place under sink conditions.

Preliminary studies using the same experimental set-up have shown that migration of both actives across the dialysis membrane and into the acceptor phase only marginally influences their overall release profiles. More specifically, when both actives are simply introduced in the dialysis membrane in an aqueous phase (neither is encapsulated), RhodB release was shown to be marginally faster than that of the encapsulated species undergoing triggered release at pH conditions higher than pH 7 (discussed in full in the results section). In addition, release of non-encapsulated DMP was approximately seven-times greater than that in the case where DMP is enclosed within the emulsion droplets. Therefore in both cases, the dominant physical phenomena and as such the rate-limiting steps driving overall co-release of the actives are the triggered

discharge of Active 1 (RhodB) from the NaCAS/CS complexes and the migration of Active 2 (DMP) across the interfacial barrier around the emulsion droplets.

### *2.2.10 Cumulative Fractional Release (CFR) profiles*

Cumulative fractional release (CFR) profiles for both releasing species are presented as a function of time *t*. CFR is calculated as the fraction of the cumulative absolute amount of active released at each time *t* interval ($M_t$) over the cumulative absolute amount of active released at infinite time ($M_\infty$); $M_\infty$ should be equal to the absolute amount of active encapsulated within the delivery system (particles or droplet) at time $t = 0$. CFR data is calculated using the following relationship:

$$CFR = \frac{M_t}{M_¥} = \frac{M_t^{sup} - M_0^{sup}}{M_{max} - M_0^{sup}} \qquad \text{Eq. 2}$$

where $M_t^{sup}$ is the total mass of active in the acceptor phase as measured at time *t*, and $M_0^{sup}$ and $M_{max}$ retain their previous meanings as defined for Eq. 1.

Release of an active from within hydrophilic polymeric devices has been proposed[59],[60] to be controlled by two physical phenomena; Fickian diffusional release and case-II relaxational release. Peppas and Sahlin[60] proposed a simple mathematical model that considers these two phenomena as additive and can be used to describe release (under sink conditions and up to a CFR value of 0.6) of an active contained within polymeric devices of any shape. CFR data for Active 1 were fitted to the Peppas-Sahlin model[60] shown below:

$$\frac{M_t}{M_¥} = k_1 t^m + k_2 t^{2m} \qquad \text{Eq. 3}$$

where the first term ($k_1 t^m$) corresponds to Fickian effects while the second term ($k_2 t^{2m}$) relates to relaxational contributions to the overall release. $k_1$ and $k_2$ are kinetic constants relating to release driven by either diffusion or relaxation; when $k_1 >> k_2$ then release is controlled by diffusion, while in those cases where $k_1 << k_2$ relaxation is primarily responsible for the transport of the active through the encapsulation device. Finally, *m* is the purely Fickian diffusion exponent; the value of the exponent relating to transport due to relaxation phenomena ($2m$) is always twice that of the Fickian diffusion exponent ($m$). Peppas and Sahlin[60] further proposed that the impact of each of the two mechanisms to the overall release profile can be assessed by calculating the fractional relaxational (R) and Fickian (F) contributions from:

$$R = \frac{\frac{k_2}{k_1} t^m}{1 + \frac{k_2}{k_1} t^m} \qquad \text{Eq. 4,} \qquad F = \frac{1}{1 + \frac{k_2}{k_1} t^m} \qquad \text{Eq. 5}$$

Similarly, release of an active entrapped within the droplets of an emulsion has been described using two limiting models.[61],[62] The first relates to situations in which the release rate is primarily

driven (limited) by the diffusion of the active through the droplet's oil core and towards the emulsion interface; active concentration along the droplet radius is in this case complex and time-dependent. The second model however relates to those cases where release behaviour is controlled by the passage of the active through the interfacial barrier that exists at the droplet surface; under these circumstances the concentration of the active within the droplet is now uniform at any given time. DMP release from the emulsions studied in this work is expected to be dominated by transferal of the active across the emulsion interface and as such it should fall under the considerations in the second of these two models (this is confirmed in the results section). A mathematical model describing the release of an active when transport across the droplet interface is the rate-limiting step has been proposed elsewhere[62] and its long-time approximation is given below:

$$\frac{M_t}{M_\infty} = 1 - \exp\left(\frac{-3k_I}{r^2}t\right) \qquad \text{Eq. 6}$$

where $k_I$ is the interfacial rate constant and $r$ the emulsion droplet radius; all other symbols retain their previous meanings. Eq. 6 can be rearranged to give:

$$\ln\left(1 - \frac{M_t}{M_\infty}\right) = \frac{-3k_I}{r^2}t \qquad \text{Eq. 7}$$

and plotting $\ln(1-(M_t/M_\infty))$ against time $t$ should yield a straight line, the slope of which can be used to directly calculate $k_I$. In the present study, DMP release was modelled using Eq. 6 and CFR data were fitted to Eq. 7 in order to calculate $k_I$ constants at different pH conditions.

## Results and Discussion

The physicochemical parameters affecting protein/polysaccharide complex formation phenomena have been well documented in literature, with the most significant contributions arising as a result of the pH environment (but also temperature and pressure conditions), the magnitude of the individual opposite charges exhibited by the two biopolymers (charge density), the total biopolymer concentration (TBC), the protein to polysaccharide ratio, ionic strength and the molecular weight and flexibility of both biopolymer species.[63],[64] In the present study, NaCAS/CS complexes were formed at pH 5 by drop wise addition of CS to NaCAS under mild stirring. At pH 5, NaCAS is negatively charged and therefore electrostatic complexation with CS, which at this acidic environment exhibits a positive ζ-potential[65], is encouraged (Figure 1). The isoelectric points for both sodium caseinate (~4.0) and chitosan (~7.5-8.0) are in agreement with values reported in literature.[66],[67] Under these pH conditions complexation takes place as a result of associative phase separation, caused by charge neutralisation interactions between the two biopolymers. The ζ-potential behaviour of the formed complexes closely resembles that of chitosan until pH values near the polysaccharide's isoelectric point are reached (Figure 1). This clearly indicates that at this CS mass fraction (0.5), the chitosan content in the system is in excess of the polysaccharide concentration required for complete charge coverage of the protein, and thus a proportion (of the chitosan) remains 'free' within the aqueous continuous phase and does not take part in electrostatic events leading to the formation of complexes. This is in agreement with a previous study[48] by the present authors, where NaCAS/CS complexes were shown to exhibit near-zero ζ-potential values only when these were formed at a CS mass fraction of approximately 0.1.

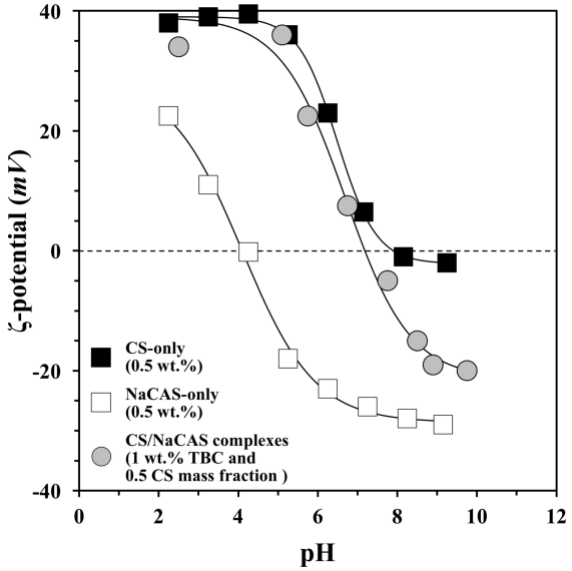


**Figure 1.** ζ-potential as a function of pH for aqueous solutions of 0.5 wt.% chitosan (CS; ■) and 0.5 wt.% sodium caseinate (NaCAS; □), and an aqueous dispersion of sodium caseinate/chitosan (NaCAS/CS; ●) complexes of 1 wt.% TBC and 0.5 CS mass fraction. All data points are mean values (n=3) and error bars represent two standard deviations of the mean; when not visible, error bars are smaller than the size of the symbols. ζ-potential data is each fitted to a sigmoid curve and shown to guide the reader's eye.

The air/water interfacial behaviour of NaCAS/CS complexes formed at different pH values provides further evidence that electrostatic interactions are more pronounced at pH 5 (Figure 2). Dynamic surface tension data for NaCAS/CS complexes of 1 wt.% TBC (data not provided here) did not show clear differences with changes to the CS mass fraction or pH and the profiles obtained were very similar to a 1 wt.% NaCAS-only system. This is because the amount of unassociated protein in these systems (although potentially varied) is high enough to 'overpower' the obtained signal corresponding to the air/water interfacial behaviour. However when the TBC was significantly lowered it was possible for differences in the dynamic surface tension profiles between NaCAS/CS complexes and their protein-only and polysaccharide-only constituents to become more evident (Figure 2). While chitosan does not exhibit any surface activity[68] and does not appear to be sensitive to the induced pH changes, sodium caseinate does cause a decrease in surface tension (reduced after 120 s to ~50 mN $m^{-1}$ at pH 7 and ~53 mN $m^{-1}$ at pH 5) with a faster rate of reduction at pH 7 than at pH 5. A previous study[69] on the adsorption of pure milk proteins ($\beta$-casein and $\beta$-lactoglobulin) at the air/water interface revealed that as the pH is lowered from pH 7 towards the isoelectric points of the two species, both protein films become thicker and thus the rate of protein diffusion to the interface (as observed in this study) would be reduced. Analysis of the data for the NaCAS/CS complexes shows that surface tension is increased as the CS mass fraction of the complexes is also increased; the more clear change observed between complexes with 0.5 (0.025 wt.% NaCAS/0.025 wt.% CS) and 0.8 (0.025 wt.% NaCAS/0.1 wt.% CS) CS mass fractions. As the NaCAS overall content remains the same the observed increase is primarily a result of electrostatic interactions between the protein and polysaccharide being further promoted due to the increasing chitosan content. As the CS mass fraction is reduced, the air/water interfacial behaviour of NaCAS/CS complexes appears to progressively approach the profile acquired for the NaCAS-only system. Finally there is also evidence of enhanced complexation at pH 5 as opposed to pH 7, with surface tension data under the latter pH conditions reaching lower equilibrium values (also at a faster rate of surface tension reduction) owing to their higher (non-complexed) protein content (Figure 2). As previously discussed, this is obviously further exacerbated by the ease by which protein diffusion to the interface takes place at pH 7 (compared to that at pH 5).[69]

It is clear that the NaCAS/CS complexation phenomena reported here are predominantly electrostatic in nature, with lesser contributions perhaps also arising due to hydrogen bonding and hydrophobic interactions. Such electrostatic complexes are typically termed coacervates and are distinctively different to complexation through covalent bonding (chemical association) between protein and polysaccharide molecules, which tends to give essentially permanent complexes, which in turn are usually characterised as conjugates.[51],[63],[64] Visualisation using light microscopy of the NaCAS/CS complexes in this study revealed structures of irregular shape, relatively large dimensions (equivalent particle diameters >100 µm) and highly polydisperse; this particle morphology was typical of NaCAS/CS complexes formed at pH 5 across the studied range of CS mass fractions (0.1-0.75) and TBCs (0.1-2 wt.%). As such, these NaCAS/CS complexes (formed under low shear mixing) are more akin to solid-like phases (i.e. co-precipitates)[64] rather than the typical liquid-like phase separated biopolymer-rich phases reported in literature as

coacervates[51],[70]. Subjecting these coarse precipitated dispersions to sonication afforded a significant reduction in particle size that was almost independent of TBC but was strongly influenced by the CS mass fraction (Figure 3). Although complexes with a CS mass fraction of 0.1 were initially reduced in size (down to ~1-3 μm) as a result of sonication, these structures ultimately re-aggregate and revert back to their original dimensions. Conversely, sonicating NaCAS/CS complexes with CS mass fractions equal or greater to 0.25 resulted in sub-micrometre particulate structures with a monomodal size distribution and reduced polydispersity (Figure 3A). Even one week following formation and sonication, these systems largely maintained their size and remained well suspended within their aqueous environment with minimal if any indication of precipitation (Figure 3B). This contrast in behaviour is directly related to the presence of a chitosan excess (in complexes with CS mass fractions $\geq 0.25$) which appears to provide sufficient electrostatic repulsion between the newly formed sub-micrometre particulates thus hindering their aggregation and ensuring that their dimensions following sonication are maintained; complexes with CS mass fractions $\geq 0.25$ have $\zeta$-potential values of ~38 mV (Figure 1) while those with a CS mass fraction of 0.1 exhibit a near-zero $\zeta$-potential value[48]. A similar behaviour has been previously reported[65] for chitosan-gellan electrostatic nano-complexes, where neutrally charged polyelectrolyte assemblies were found (soon after formation) to aggregate into species of larger sizes.

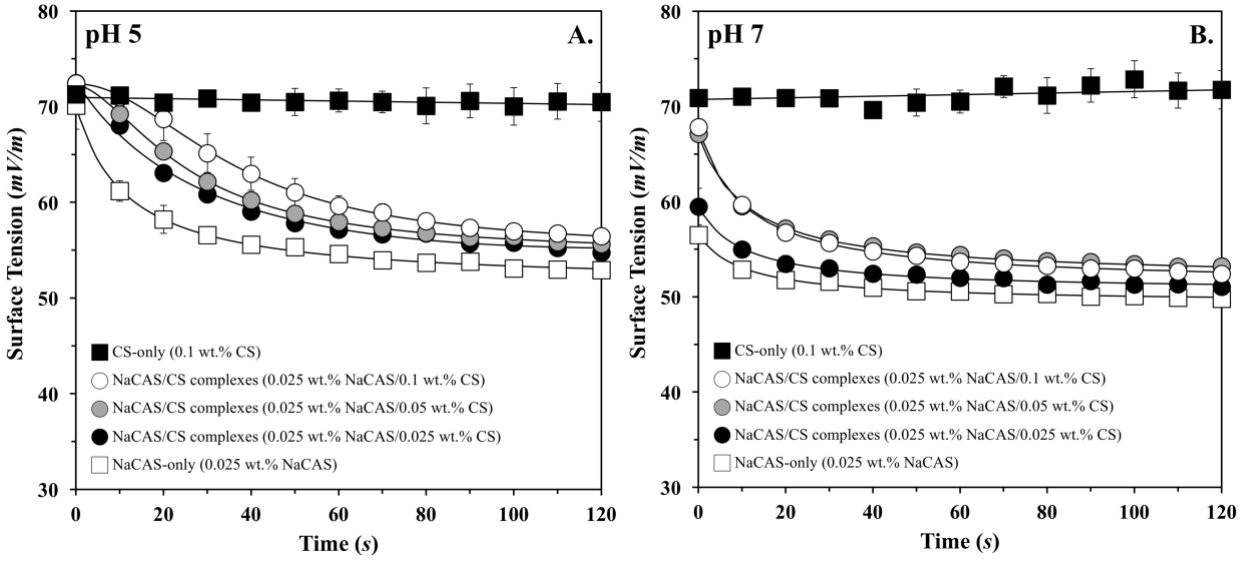


**Figure 2.** Dynamic surface tension profiles for chitosan (CS), sodium caseinate (NaCAS) and sodium caseinate/chitosan (NaCAS/CS) complexes as a function of pH environment; **A.** pH 5 and **B.** pH 7. Data shown are for 0.1 wt.% CS-only (■) and 0.025 wt.% NaCAS (□), and NaCAS/CS complexes of 0.025 wt.% NaCAS/0.1 wt.% CS (0.8 CS mass fraction; ○), 0.025 wt.% NaCAS/0.05 wt.% CS (0.66 CS mass fraction; ●) and 0.025 wt.% NaCAS/0.025 wt.% CS (0.5 CS mass fraction; ●). All data points are mean values (n=3) and error bars represent two standard deviations of the mean; when not visible, error bars are smaller than the size of the symbols. Solid lines/curves are shown to guide the reader's eye.

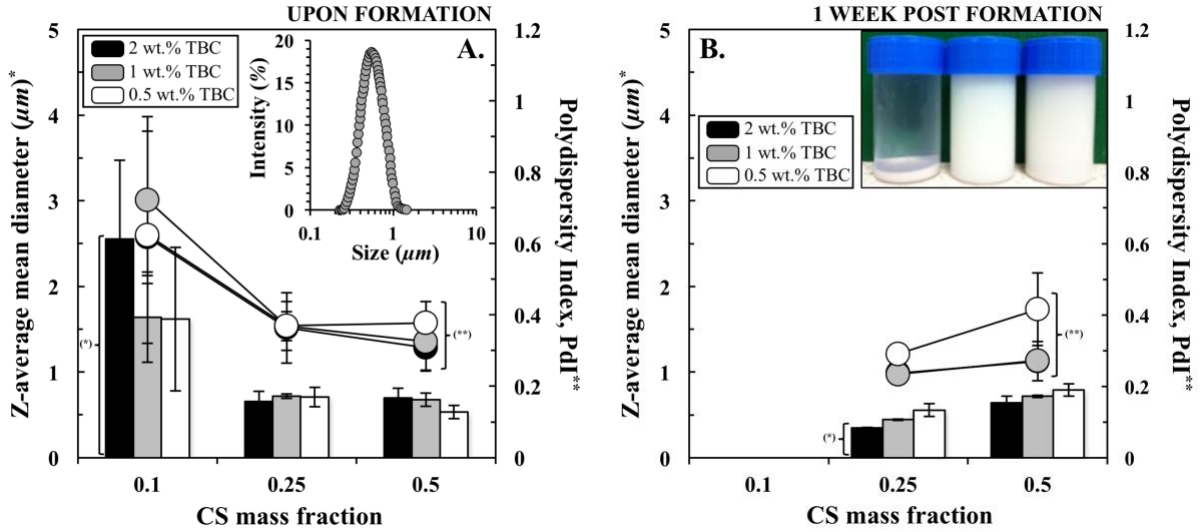


**Figure 3.** Z-average mean diameters (bars) and polydispersity indices (circles) for sodium caseinate/chitosan (NaCAS/CS) complexes of varying TBC and CS mass fractions (**A**) following sonication and (**B**) after 1 week of storage. Also shown, the particle size distribution obtained by DLS for NaCAS/CS complexes of 1 wt.% TBC and 0.5 CS mass fraction upon formation and subsequent sonication (**inset A**), and the visual appearance of aqueous suspensions of NaCAS/CS complexes of 1 wt.% TBC at CS mass fractions (from left to right) of 0.1, 0.25 and 0.5 one week following formation and subsequent sonication (**inset B**). All data points are mean values (n=3) and error bars represent two standard deviations of the mean; when not visible, error bars are smaller than the size of the symbols. Trendlines are shown to guide the reader's eye.

In this part, the encapsulation of a hydrophilic fluorescent dye, fluorescein sodium salt (FSS), within the NaCAS/CS complexes formed at pH 5 was studied. FSS has been previously used as a model active[48] and is commonly employed as a charged drug mimetic.[71],[72] In the present study, it was envisaged that FSS would be electrostatically attracted to the cationic amine groups on the chitosan backbone, as well as to the cationic amino acid residues on sodium caseinate.[73] Nonetheless, the size and ζ-potential of (sonicated) NaCAS/CS complexes does not seem to be affected by the presence of FSS, with both these properties only marginally influenced (for a fixed TBC) by the CS mass fraction (Figure 4).

The effect of the TBC and CS mass fraction of the formed NaCAS/CS complexes (which were subsequently sonicated) were also investigated with respect to the fractional encapsulation efficiency (FEE) of FSS. FEE values were determined by following a protocol, where the dispersions of FSS-containing NaCAS/CS complexes were centrifuged over different timescales and the absorbance of the supernatant was measured using UV-VIS spectroscopy. These measurements were performed to ensure interferences from soluble complexes and unseparated particles did not compromise accurate FSS quantification; for example, a dispersion of FSS-containing NaCAS/CS complexes of 2 wt.% TBC had to be centrifugation for 150 minutes at 20,000 rpm for a stable absorbance reading to be achieved. The FEE of the NaCAS/CS complexes does not seem to be effected by sonication and the originally achieved encapsulation efficiencies remain unchanged (Figure 4) despite the significant reduction in size. This has been previously[48] suggested to further confirm that the FSS is anchored onto the colloidal structure of the NaCAS/CS

complexes predominantly through electrostatic forces. The dependency of the FEE on the CS mass fraction in the NaCAS/CS complexes however is very clear, with encapsulation efficiency being reduced as the chitosan fraction is increased (Figure 4). Earlier work[48] has reported that FSS can also be encapsulated (at pH 5) during the formation of NaCAS- and BSA-only protein aggregates (CS mass fraction of 0); nonetheless the same investigation noted that the presence of chitosan was necessary in order to form stable colloidal suspensions upon sonication. It thus appears that the reduction in FEE is mainly driven by the decrease in the NaCAS content (as the CS fraction is increased) and that the extent of the NaCAS-FSS and NaCAS-CS competitive electrostatic interactions could heavily influence the encapsulation capacity of the formed complexes. Although beyond the scope of the present study, further work to fully understand the physical phenomena involved in the encapsulation of FSS in NaCAS/CS complexes is required.

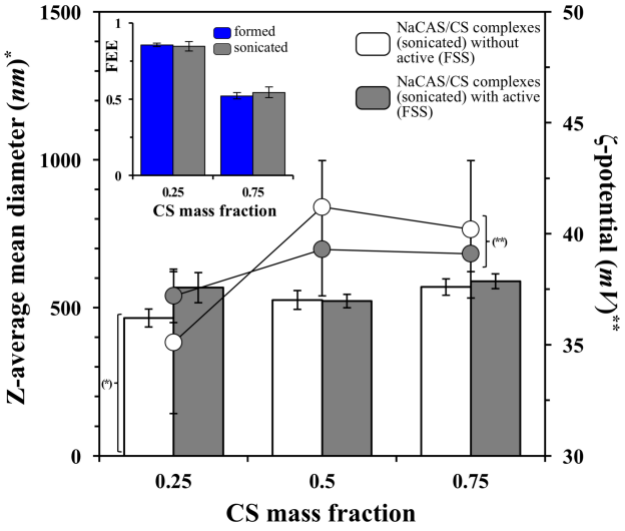


**Figure 4.** Z-average mean diameter (bars) and ζ-potential (circles) for sodium caseinate/chitosan (NaCAS/CS) complexes of 1 wt.% TBC as a function of CS mass fraction. Data presented in the main graph is for sonicated complexes without (empty bars or circles) or with (grey bars or circles) encapsulated fluorescein sodium salt (FSS). Inset graph shows the fractional encapsulation efficiency (FEE) of FSS within complexes either immediately formed (blue bars) or then also sonicated (grey bars). All data points are mean values (n=3) and error bars represent two standard deviations of the mean. Trendlines are shown to guide the reader's eye.

For sonicated NaCAS/CS complexes, encapsulation efficiency was strongly dependent on the TBC (with CS mass fraction and FSS loading both constant) and FEE was found to increase from approximately 0.7 to 0.9 as TBC was taken from 0.5 to 2 wt.% (Figure 5). As the size of the NaCAS/CS complexes (CS mass fractions ≥ 0.25) does not change with TBC (Figure 3A), the elevated biopolymer content will result in an increase in the number of these co-precipitates, which in turn can enhance the FEE of the system as further 'compartments' for FSS encapsulation will now be available. In addition, FEE was also found to vary with the FSS loading that was initially introduced in the system (Figure 5), with FSS encapsulation efficiency slightly reducing as the amount of active is increased from 20 to 80 μg $g^{-1}$. For a fixed TBC, increasing the amount of

active in the system would add further strain in terms of encapsulation capacity upon the same (in terms of number) population of NaCAS/CS complexes, which in response exhibit a reduced encapsulation efficiency. This is in agreement with a previous study[48] on the encapsulation capacity of chitosan/carrageenan hydrogel beads; the encapsulation efficiency of these (non-cross-linked) polyelectrolyte complex beads was found to decrease with increasing active (sodium diclofenac) loading.

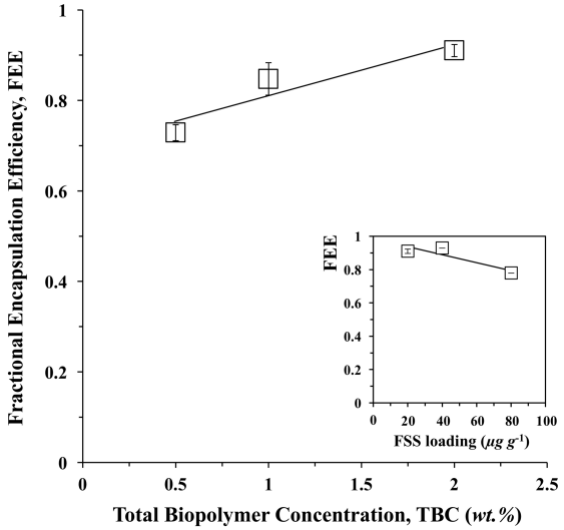


**Figure 5.** Fractional encapsulation efficiency (FEE) of fluorescein sodium salt (FSS) within sodium caseinate/chitosan (NaCAS/CS) complexes as a function of total biopolymer concentration, TBC (NaCAS/CS complexes of 0.25 CS mass fraction and 20 μg $g^{-1}$ FSS loading). Inset graph shows FEE as a function of FSS loading (NaCAS/CS complexes of 0.25 CS mass fraction and 2 wt.% TBC). All data points are mean values (n=3) and error bars represent two standard deviations of the mean. Linear trendlines are shown to guide the reader's eye.

The response of NaCAS/CS complexes formed at pH 5, in terms of their encapsulation capacity, dimensions (mean particle diameter) and charge (ζ-potential), to changes in the pH environment was also studied (Figure 6). FSS- or RhodB-containing NaCAS/CS complexes of 1 wt.% TBC and 0.25 CS mass fraction, initially formed at pH 5 with a FEE value of 0.85, where analysed under pH conditions ranging from approximately pH 2 to pH 11. Due to its acid-base chemistry it was not possible to measure FSS content at pH values below pH 5 and as such RhodB was used to monitor active entrapment/release at these acidic conditions; in general, FEE values for RhodB were comparable to those for FSS for all NaCAS/CS complexes studied here and those previously reported[48]. The mean diameter and ζ-potential data shown in Figure 6 further confirm the strong relationship between electrostatic interactions and the structure of the NaCAS/CS co-precipitated complexes. At ~pH 6 and below, the size of the NaCAS/CS complexes as initially formed at pH 5 (and then sonicated) is maintained (at approximately 600 nm), supported by the prevalence of attractive electrostatic interactions between the protein and polysaccharide constituents; note that the ζ-potential profile shown here for NaCAS/CS complexes of 1 wt.% TBC and 0.25 CS mass fraction (Figure 6) closely follows the one for complexes at the same TBC but a CS mass fraction

of 0.5 (Figure 1). As the pH environment shifts to ~pH 7 and above, electrostatic interactions become weaker and NaCAS/CS complexes appear to swell and increase to approximately 2 µm in mean diameter (Figure 6); this corresponds to a volume change for the NaCAS/CS complexes of approximately 3600%. Optical microscopy was used to confirm that the measured increase in the size of the complexes was not due to flocculation. However, as demonstrated by the larger error bars in the average mean diameter data collected above pH 7, the extent of swelling exhibited by the NaCAS/CS complexes appears to be relatively random. It has been proposed[74] that the electrical characteristics of the different molecular constituents of mixed biopolymer assemblies can significantly alter the structure of these complexes, leading to swelling or shrinking depending on changes to environmental cues such as pH or ionic strength.

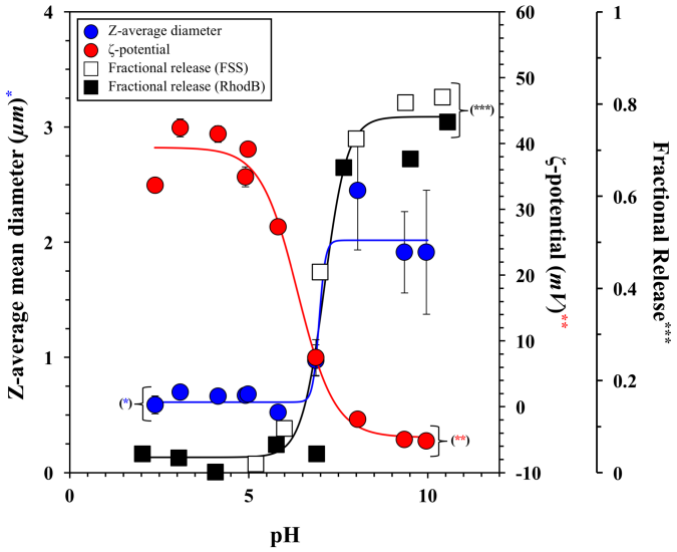


**Figure 6.** Z-average mean diameter (●), ζ-potential (●) and fractional release (FSS:□, RhodB:■) for sodium caseinate/chitosan (NaCAS/CS) complexes of 1 wt.% TBC and 0.25 CS mass fraction (initially formed at pH 5 with 0.85 FEE) as a function of changes to pH environment. Fractional release data only show the amount of liberated material that was initially encapsulated. All data points are mean values (n=3) and error bars represent two standard deviations of the mean; when not visible, error bars are smaller than the size of the symbols. Z-average mean diameter, ζ-potential and fractional release data are each fitted to a sigmoid curve, shown to guide the reader's eye.

Having already shown (Figure 2) to exhibit a level of interfacial activity (primarily driven by their protein content), the capacity of the NaCAS/CS co-precipitated complexes to provide Pickering emulsion stability was also investigated. A series of o/w (20/80 wt.%) emulsions exclusively stabilised by colloidal NaCAS/CS complexes fabricated with a fixed TBC of 1 wt.% and varied CS mass fractions, were prepared (at pH 5, corresponding to the acidic environment used to induce protein-polysaccharide complexation) and monitored, in terms of their droplet size, over a 2-month period (Figure 7). In addition to these, o/w emulsions stabilised by either the NaCAS or CS species alone, both at a concentration of 1 wt.% (corresponding to the TBC of the complexes), were also studied. All emulsion systems were formulated in the presence of both

active-containing (FSS or RhodB) and non active-containing NaCAS/CS co-precipitates in order to identify the impact of encapsulated species upon the capacity of their carriers to impart Pickering stabilisation.

Despite exhibiting clear evidence of droplet flocculation and some level of protein aggregation, emulsions stabilised by NaCAS alone show very good stability against droplet coalescence (Figure 7). Under pH conditions close to the protein's isoelectric point (pH 5), the repulsive forces between emulsion droplets, as induced by protein adsorption at the interface, are significantly weakened, resulting in droplet aggregation or, in certain cases, the formation of a three-dimensional gel network.[75] Although it has been shown in the past that encapsulation can be achieved in NaCAS-only solutions at pH 5, mainly due to the formation of protein aggregates, this is beyond the scope of the present study and as such was not investigated further.[48] It is worth noting that the same study[48] concludes that although encapsulation is indeed possible in the absence of CS, the active-containing protein precipitates formed are quite large (> 100 μm) and do not exhibit colloidal stability once their size is reduced by sonication. On the other hand, emulsions stabilised by CS alone are extremely unstable with complete phase separation for all systems taking place soon after their formation (Figure 7). This is not surprising as chitosan, previously shown here to lack interfacial activity (Figure 2), is rarely recognised in literature as a polysaccharide of acceptable emulsification properties.[76] Although there have been some reports on the capacity of chitosan to produce stable o/w emulsions on its own, this has been attributed to the increase in the viscosity of the aqueous matrix phase induced by the dissolution of chitosan rather than to the polysaccharide's interfacial activity.[77]

In the case of emulsions stabilised by NaCAS/CS co-precipitated complexes the key factor affecting the size of the produced oil droplets and moreover their long-term stability, appears to be the CS mass fraction employed in the fabrication of these biopolymer constructs (Figure 7). Complexes with chitosan mass fractions up to (and including) 0.5 were able to facilitate the formation of emulsion droplets with average diameters of approximately 11 μm (CS mass fractions of 0.25) and 8 μm (CS mass fractions of 0.5). Emulsion droplet size was marginally dependent on CS mass fraction (0.25 or 0.5) or the presence of encapsulated FSS, however emulsions stabilised by RhodB-containing complexes were found to have smaller droplet sizes. Upon formation, emulsions exhibited evidence of flocculation (Figure 7), which following storage is suggested to result in the apparent increase in the droplet sizes for all systems. Emulsions stabilised by protein/polysaccharide complexes have been previously shown to be susceptible to flocculation. In recent studies it was specifically shown that emulsions stabilised through interfacial complexation between proteins and polysaccharides are particularly prone to flocculation events, while this type of instability is greatly reduced (although still present) when the biopolymers have undergone complexation prior to emulsion formation.[54],[78] With reference to the present work, emulsions stabilised by complexes at these intermediate to low chitosan mass fractions (≤0.5) also exhibited creaming, which is expected to promote flocculation phenomena between droplets present in the cream layer as these are subjected to prolonged periods of droplet-to-droplet contacts. The observed level of droplet aggregation (especially in the case of emulsions stabilised

by complexes with a CS mass fraction of 0.5) appears to be almost unaffected by the presence of the encapsulated load within the biopolymer particulates. It is important to note that these emulsion systems (chitosan mass fractions ≤ 0.5), although prone to flocculation events, were still found to maintain an emulsion microstructure that largely resists coalescence and does not display any evidence of phase separation. Despite their reduced protein content, complexes of a higher CS mass fraction (0.75) were able to provide emulsions with slightly smaller droplets; ~5 μm in diameter (Figure 7). Both FSS- and RhodB-containing complexes provided emulsions of similar droplet sizes to systems stabilised by the non active-containing co-precipitates. In all cases, emulsions exhibited excellent stability with no coarsening observed over the 2-month storage period (Figure 7). The obtained micrographs for these systems (Figure 7) suggest that, although perhaps not absent, flocculation events have lessened significantly in comparison to the obvious floc formation seen at lower CS mass fractions. Any flocs formed in emulsions stabilised by complexes with a high CS mass fraction (0.75) are now expected to be weaker and therefore easily dissociated during droplet size analysis in the dispersion cell of the laser diffraction equipment. The greatly reduced flocculation phenomena as well as the reduction in the rate of creaming in these systems, are both expected to be driven by the high(er) level of non-adsorbed chitosan present at this CS mass fraction.

It is worth considering the nature of the species providing interfacial stabilisation to the o/w emulsions studied here. Previous work[48] on NaCAS/CS complexes has demonstrated that these colloidal entities exhibit near-zero z-potential values when formed at a CS mass fraction of approximately 0.1. As such it is valid to anticipate that aqueous dispersions of NaCAS/CS co-precipitates formed at higher CS mass fractions (such as those utilised in the present study; CS mass fractions equal or greater than 0.25) would include minimal non-complexed amounts of (free) protein. This hypothesis is further substantiated by the dynamic surface tension data presented in Figure 2. Although the presence of free NaCAS cannot be completely dismissed, it is clear that as the CS mass fraction increases dynamic surface tension is reduced at a lower rate and to higher equilibrium value. It is therefore clear that when the aqueous dispersions of these complexes are used to form emulsions, interfacial stabilisation would predominantly occur due to the adsorption of the NaCAS/CS co-precipitates. Although any contribution arising from the presence of free NaCAS cannot be entirely ignored, there is strong evidence to suggest that the stability of the oil/water interfaces is principally due to the NaCAS/CS complexes. What is more, the interfacial dominance of the complexes is also expected to be enhanced as their CS mass fraction is increased.

In classical Pickering theory, adsorbed molecular species are predicted to modify particle wettability[40], which is a key parameter influencing both emulsion formation and subsequent long-term stability. Yet, the overarching conclusion for the NaCAS/CS co-precipitates studied here, is that the observed Pickering functionality can be tailored/promoted by only considering the structure and composition of the particles themselves rather than whether these also act as carriers of an active component. The precise manner by which these two formulation parameters can influence the wettability of the NaCAS/CS particles was not investigated as part of the present study.

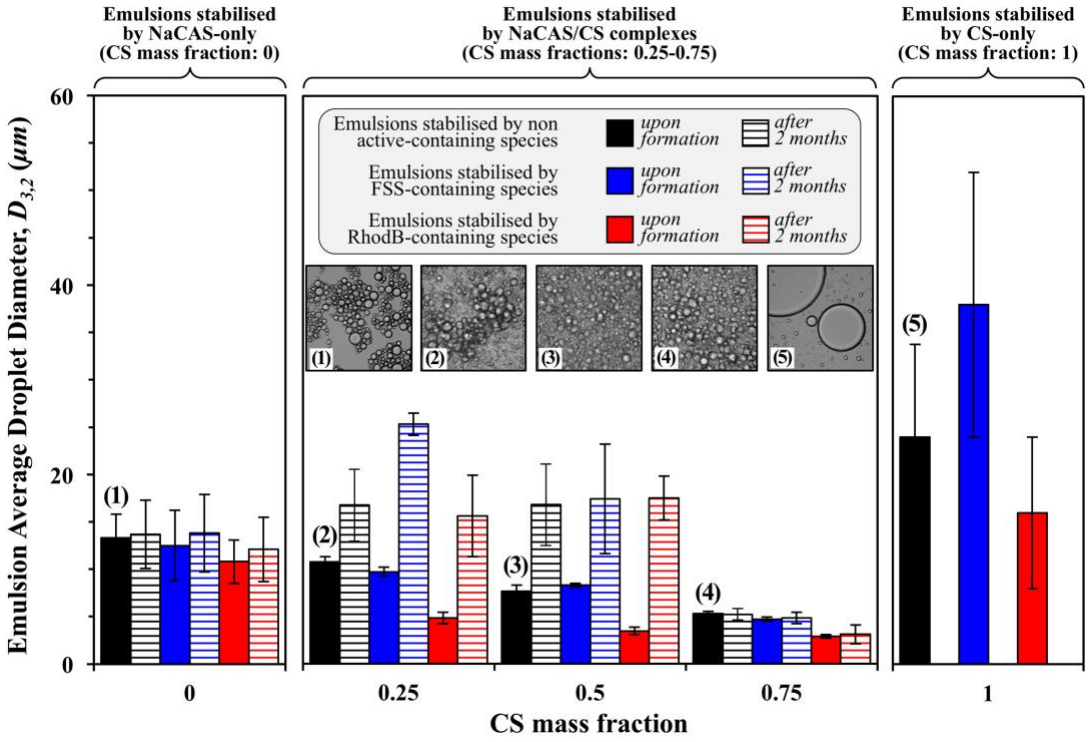


**Figure 7.** Average droplet diameters ($D_{3,2}$) of simple o/w (20/80 wt.%) emulsions (upon formation and following 2 months of storage) stabilised by non active- (■) and active-containing (FSS:■ or RhodB:■) sodium caseinate/chitosan (NaCAS/CS) complexes of 1 wt.% TBC as a function of CS mass fraction. CS mass fractions of 0 denote emulsions stabilised solely by NaCAS, while CS mass fractions of 1 denote CS-only stabilised emulsions. Inset light microscopy images show emulsion microstructures as initially formed in the presence of non active-containing NaCAS/CS complexes with CS mass fractions of: **(1)**: 0, **(2)**: 0.25, **(3)**: 0.5, **(4)**: 0.75, and **(5)**: 1; the width of all micrographs corresponds to approximately 150 μm. All data points are mean values (n=3) and error bars represent two standard deviations of the mean; when not visible, error bars are smaller than the size of the symbols.

The demonstrated dual capacity of the NaCAS/CS complexes to facilitate the encapsulation of an active species while at the same time providing emulsion stability was utilised to investigate the co-encapsulation of two active components within a simple o/w emulsion microstructure. More specifically, these bi-functional protein/polysaccharide complexes were used to encapsulate RhodB (Active 1), while PE (Active 2) was loaded into the oil droplets of the emulsion that these biopolymer assemblies stabilise. It was therefore envisaged that although the two incompatible model actives (RhodB and PE representing a hydrophilic and a hydrophobic model active load, respectively) would co-exist within the same overall system, they would be actually encouraged to occupy discrete parts of the formed emulsion microstructure; RhodB would be expected to follow the NaCAS/CS complexes and reside at the interface while, due to its hydrophobic nature, PE would largely remain contained within the oil droplets of the emulsion. Using this approach, an o/w emulsion, stabilised by sodium NaCAS/CS complexes (formed at pH 5) of 1 wt.% TBC and a CS mass fraction of 0.25, was loaded with RhodB and PE and the anticipated segregated co-encapsulation of these two model actives at pH 5 was confirmed using confocal microscopy (Figure 8). RhodB and PE have minimal overlapping excitation and emission spectra, thus

facilitating independent visualisation via separate monitoring of their fluorescence emissions; in the obtained micrographs, RhodB (Active 1) and PE (Active 2) appear green and blue, respectively.

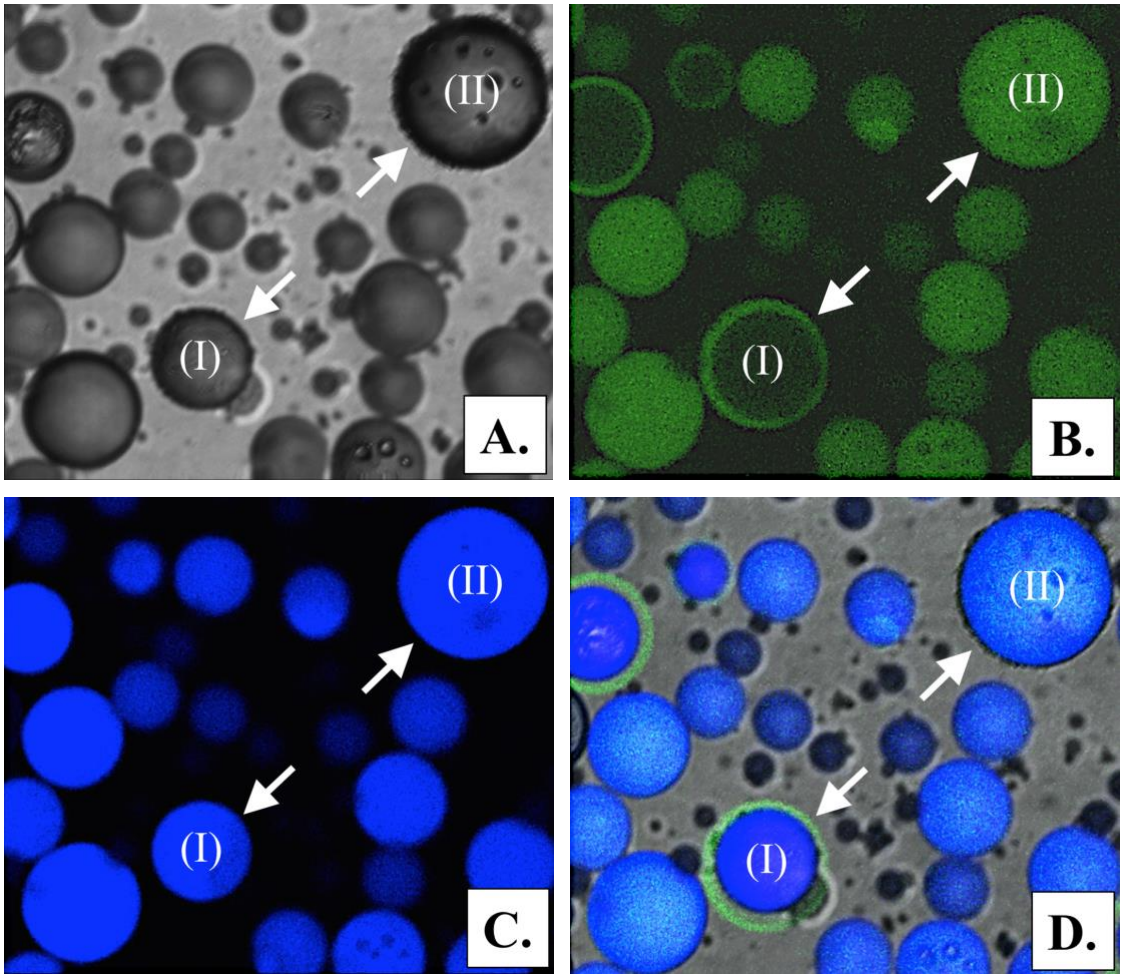


**Figure 8. A.** Optical microscopy image of an o/w emulsion (at pH 5) stabilised by sodium caseinate/chitosan (NaCAS/CS) complexes of 1 wt.% TBC and 0.25 CS mass fraction (initially formed at pH 5). **B.** Fluorescent emission (green) from RhodB (Active 1) encapsulated within the NaCAS/CS complexes. **C.** Fluorescence emission (blue) from PE (Active 2) encapsulated within the emulsion droplets. **D.** Combined fluorescence emissions from the two Actives demonstrating the emulsion's co-encapsulation capacity. Droplet (I) is situated on the micrograph's focal plane, while droplet (II) is situated below the focal place. The width of all micrographs corresponds to approximately 250 μm.

The confocal micrographs of the o/w microstructure presented in Figure 8 show the fluorescent emission from RhodB alone (Figure 8B), PE alone (Figure 8C), and finally the RhodB and PE combined emissions (Figure 8D). Both RhodB (particle-contained) and PE (emulsion droplet-contained) are mainly associated with the interface and dispersed phase of the emulsion and neither of the two actives appears to be present in any large extent within the continuous phase of the system. In view of the high fractional encapsulation efficiency exhibited by the NaCAS/CS co-precipitates (at 1 wt.% TBC and a CS mass fraction of 0.25; Figure 4 and Figure 5) and their

capacity to retain RhodB at pH 5 with minimal release (Figure 6), it is not surprising that confocal microscopy indicates that only a minimal amount of the model hydrophilic active is present in the continuous phase of the formed emulsions. Similarly, the absence of PE from the aqueous phase is expected as the solubility of the model hydrophobic active in water is negligible.[79] In those cases where the focal plane in the combined fluorescent emissions micrograph (Figure 8D) corresponds to a cross-sectional area of a dispersed phase entity (for example droplet (I)), a 'halo' of RhodB fluorescent emission can be observed to surround a 'reservoir' of PE emission, originating from the disperse phase of the emulsion. Although co-encapsulation can be confirmed for all visible droplets from the micrographs of the separate emission spectra for the two actives (Figure 8B and C), the optical 'halo' effect shown for droplet (I) is not apparent for emulsion droplets situated below the focal plane of the obtained confocal micrograph (for example droplet (II)). Overall, confocal microscopy successfully confirmed that segregated co-encapsulation of two actives within a simple o/w emulsion can be achieved, with the actives, as anticipated, being partitioned within well-defined domains of the fabricated simple emulsion microstructure.

The co-release of RhodB (Active 1, hydrophilic) and DMP (Active 2, hydrophobic), co-encapsulated within o/w emulsions stabilised by NaCAS/CS complexes (at 1 wt.% TBC and a CS mass fraction of 0.25), was subsequently investigated. The produced emulsions were placed inside semi-permeable cellulose dialysis membranes that were submersed into an external aqueous phase at pH 3, 5, or 10 and the co-release of both RhodB and DMP was monitored through absorbance measurements of samples collected from the acceptor phase at appropriate timescales over a period of 48 hours; the obtained results are presented in Figure 9. The findings presented here clearly demonstrate that co-release of both model actives is achievable and what is more the two encapsulated species are liberated over markedly different timescales and through quite independent release mechanisms. Release of RhodB (Active 1; encapsulated within the bi-functional NaCAS/CS co-precipitates stabilising the oil-water interface) is closely associated with changes to the magnitude of electrostatic interactions within the biopolymer carriers as induced by the pH environment. At pH values akin to those used to induce protein/polysaccharide complexation (pH 5), and thus NaCAS/CS particle fabrication and Active 1 encapsulation, or lower (pH 3), RhodB release is negligible (Figure 9A and B). However at pH 10, release of RhodB is no longer constrained and the triggered discharge of the hydrophilic species now takes place (Figure 9C). The co-release of RhodB from the o/w emulsions stabilised by NaCAS/CS complexes practically matches the release of RhodB alone from aqueous dispersions of the protein/polysaccharide co-precipitates, reported earlier in this study. The sodium caseinate/chitosan complexes (as aqueous suspensions and not within an emulsion microstructure) were shown to retain their structure and furthermore prevent the release of an encapsulated hydrophilic active (RhodB or FSS), up to pH 6 (Figure 6). These biopolymer complexes were then shown to swell as the magnitude of the electrostatic forces (present at pH 6 and below) is diminished at pH values above the pKa of chitosan (pH = 6.5-7.0), (Figure 6), thus expanding their original electrostatically-maintained structure and to a large extent losing their ability to encapsulate the active, which is then almost immediately released (Figure 9C).

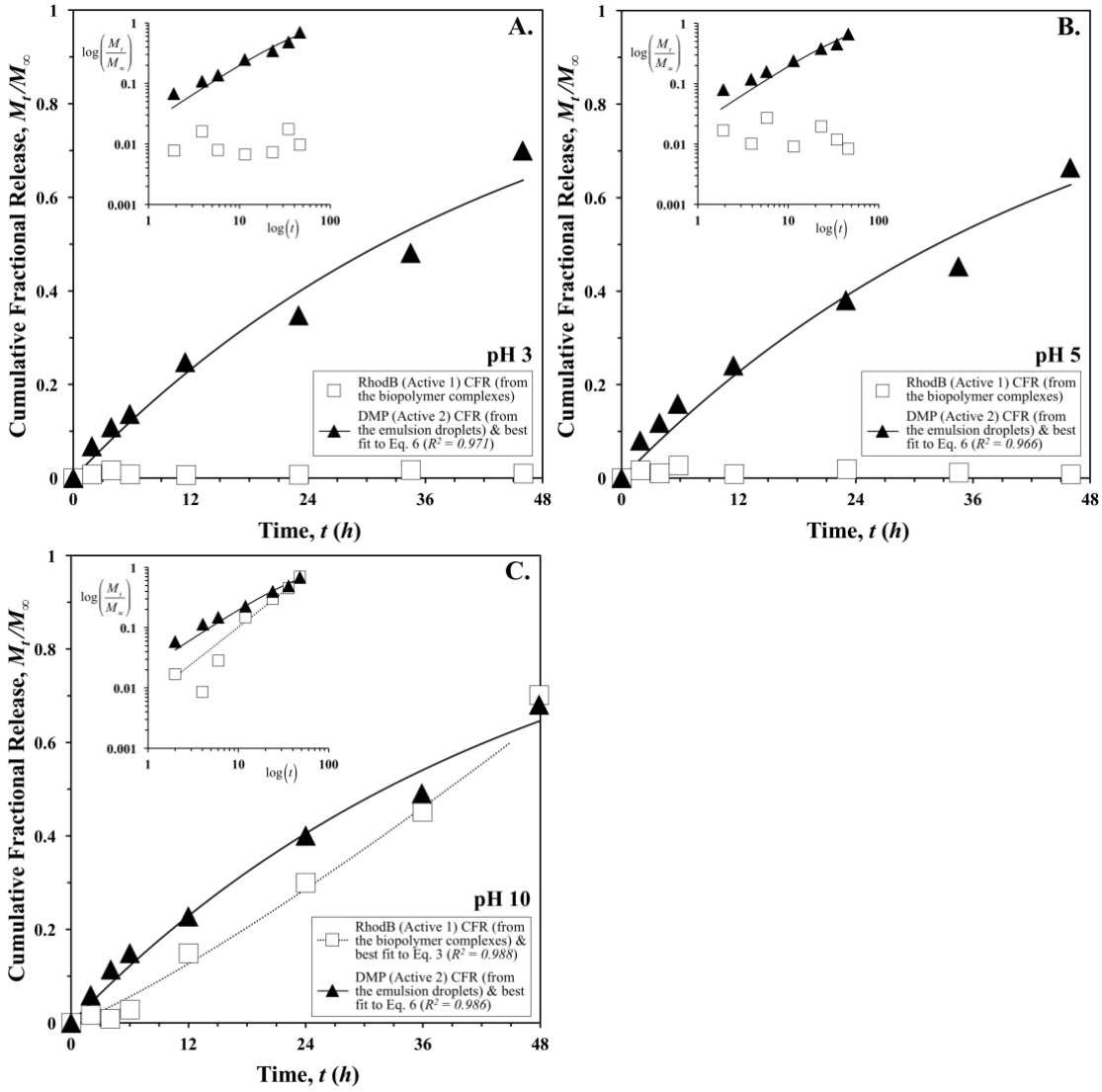


**Figure 9.** Co-Release (Cumulative Fractional Release, CFR) profiles for Active 1 (RhodB: □) and Active 2 (DMP: ▲) from simple oil-in-water emulsions stabilised by sodium caseinate/chitosan (NaCAS/CS) complexes of 1 wt.% TBC and 0.25 CS mass fraction (initially formed at pH 5 with 0.85 FEE) as a function of pH conditions; **A.** pH 3, **B.** pH 5, and **C.** pH 10. The best fits of CFR profiles for RhodB (····), encapsulated within the NaCAS/CS complexes, to Eq [3] and for DMP (—), contained within the emulsion droplets, to Eq [5] are also presented. Inset graphs show CFR profiles for both actives across the different pH environments on a log-log scale.

The CFR data for the co-release of RhodB and DMP were fitted to the semi-empirical Peppas-Sahlin model[60] (Eq. 3) and to a model proposed by Guy and co-workers[61] (Eq. 6), respectively; the best fits of the CFR profiles for both actives to these models are shown in (Figure 9). In the case of RhodB (Active 1), CFR data only at pH 10 were fitted to the Peppas-Sahlin model since at pH 3 and pH 5 no release is effectively taking place. The fit resulted in a value for the exponent $m$ of 0.589 (with release from a spherical polymeric device as a result of pure Fickian diffusion in theory corresponding to an exponent of 0.43)[60] and kinetic constants with $k_1 << k_2$. Therefore the model clearly suggests that relaxation is by far the primary mechanism responsible for the release

of RhodB from the NaCAS/CS co-precipitated complexes. The fractional relaxational (R) and Fickian (F) contributions to the overall release of RhodB were also calculated (Eqs. 4 and 5) and are presented as a function of time in Figure 10. Within the timescales of the co-release experiments (denoted by the shaded area in Figure 10) the model shows that fractional contribution due to relaxation (case II transport) approaches unity, while the Fickian contribution is practically zero. It is interesting to note that diffusion is shown to be a contributing mechanism for release only if the model is extended towards significantly smaller timescales. However according to the model this will take place for times in the order of microseconds (the relaxational and Fickian mechanisms are shown to have an equal contribution towards release at approximately 20 $\mu s$), which are obviously extremely far-removed from the experimental capabilities in the present study. Although it is unreasonable to trust the validity of such quantitative information, it is potentially safe to assume that the dominance of relaxational release (for the system at pH 10) is established relatively quickly. Case-II (relaxational) release in hydrophilic polymer devices is a transport mechanism that relates to stresses and state-transition events that occur when these structures are placed within an aqueous environment where they tend to swell.[59],[60] A recent study[80] on the swelling and deswelling of a pH-responsive electrostatically stabilized poly[2-(diethylamino)ethyl methacrylate] microgel (adsorbed to silica surfaces) has shown that such events (driven by changes to the pH environment) take place rather rapidly; swelling was found to be completed in less than 3 s, while deswelling took just over 100 s. It therefore appears that co-release of RhodB at pH 10 is driven by relaxation of the NaCAS/CS co-precipitated complexes as they swell (see Figure 6) in response to the pH change.

In general, release of an active entrapped within the droplets of an emulsion has been described using two limiting models.[61],[62] The first model is applicable to release rates that are primarily driven (limited) by the diffusion of the active through the oil phase within the emulsion droplets and towards the interface. The second one however relates to those cases where diffusion through the oil is not limiting and release behaviour is primarily controlled by the passage of the active through the interfacial barrier that exists at the droplet surface. Fitting the CFR data for the co-release of DMP to the diffusion-limited model[61] resulted in diffusion coefficients (under all three pH conditions) with an approximate value of $4.5\ 10^{-15}\ m^2s^{-1}$. However, using the Stoke-Einstein equation, the diffusion coefficient of DMP within sunflower oil (a relatively small molecule diffusing through a liquid phase of moderate viscosity) can be estimated to have a significantly lower value of $8.5\ 10^{-12}\ m^2s^{-1}$. As such, the diffusion-limited model is not applicable to the release behaviour observed in this study and instead the CFR data for the co-release of DMP were fitted to a model assuming that overall transport of the active is controlled by the nature of the interfacial layer (Eq. 6); the best fits of the CFR profiles to the interface-limiting model initially proposed by Guy and co-workers[61] are shown in (Figure 9). By rearranging the model to Eq. 7, the interfacial transport rate constants ($k_I$) for DMP co-release under each of the considered pH conditions were calculated. As the CFR profiles under all pH environments were very similar, the interfacial transport rate constants were also close and in the order of $11\ nm^2s^{-1}$ (Figure 10). A study[62] on the release of model hydrophobic solutes from submicron triglyceride emulsions reported

interfacial transport rate constants within the range of 4.5 - 45 $nm^2s^{-1}$ (for the release of capric acid) and concluded that $k_I$ values are mainly affected by the interfacial layer structure (e.g. interfacial thickness) rather than the molecular weight of the used emulsifier. Trotta[81] studied the release of indomethacin initially contained within lecithin-based microemulsions which, following dilution into an aqueous release medium, underwent composition-specific transformations into (macro)emulsions, liquid crystals, or remained as microemulsions. The calculated transfer rate constants had a wide range of values (0.08-1020 $nm^2$ $s^{-1}$), which depended on the available interfacial area (micro- versus macroemulsions) and the type of colloidal system following dilution (emulsion versus liquid crystals).[81] The $k_I$ values calculated here are comparable to those reported in literature and appear to be almost two orders of magnitude lower than those for emulsions stabilised by low molecular weight surfactants (e.g. lecithin[62]). Therefore the NaCAS/CS complexes offer a substantial interfacial barrier for the migration of DMP into the continuous phase that persists even under pH conditions (pH 10) where these co-precipitates are expected to swell. In an ongoing study, the authors are showing that the barrier provided by the NaCAS/CS complexes is also greater than the interfacial hindrance arising from the adsorption of NaCAS alone; the $k_I$ value for DMP release is approximately 30% higher for a NaCAS-stabilised interface as compared to one stabilised by NaCAS/CS complexes (data not shown here).

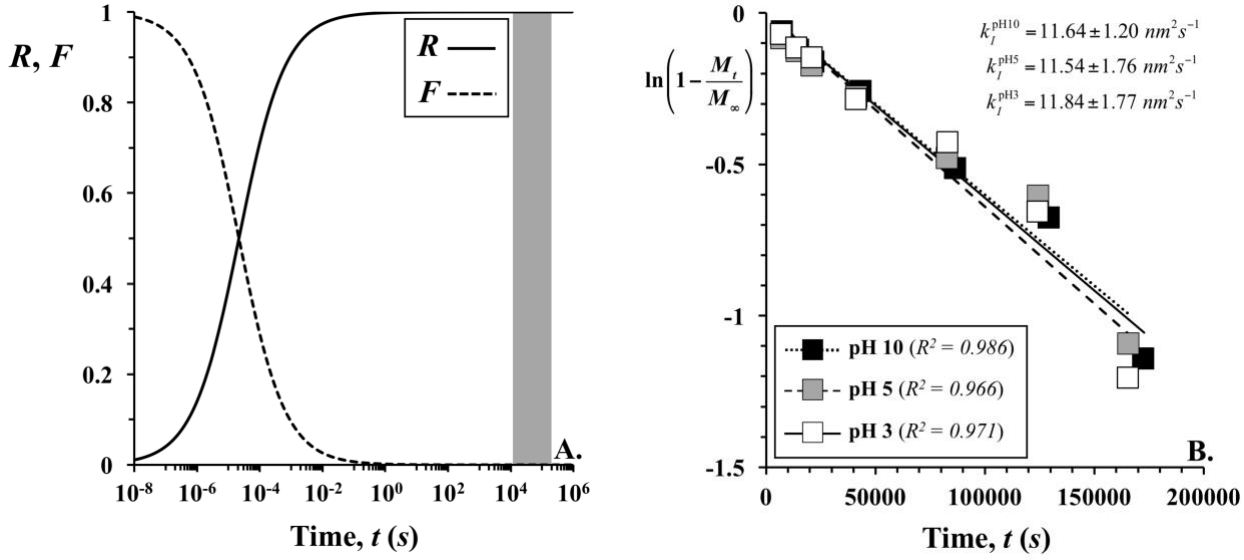


**Figure 10. A.** Relaxational (*R*) and diffusional (*F*) contributions (Eqs. 4 and 5, respectively) to the Cumulative Fractional Release (CFR) profile (shown in Figure 8) for Active 1 (RhodB), encapsulated within the sodium caseinate/chitosan (NaCAS/CS) complexes, at pH 10 as a function of time; shaded area represents the timescales over which experimental CFR data were collected. **B.** Interfacial transport rate constants ($k_I$) for Active 2 (DMP), contained within the emulsion droplets, as a function of pH environment. Interfacial transport rate constants obtained by best fits of Eq. 7 to the DMP CFR profiles (shown in Figure 9); pH 3 (□), pH 5 (▒) and pH 10 (■).

## Conclusions

The present study demonstrates that NaCAS/CS co-precipitated complexes, previously employed for the encapsulation of hydrophilic model actives and their subsequent pH-triggered release, can additionally adsorb at the oil-water interface and therefore be used to stabilise simple o/w emulsions via a 'Pickering-like' mechanism. It is shown that whether the NaCAS/CS assemblies contain an active (FSS or RhodB) or not, does not impact on their capacity to provide stable emulsions, a functionality that is primarily driven by the protein-to-polysaccharide composition used for their assembly (exemplified here as their CS mass fraction). The current work progresses to further demonstrate that these bi-functional co-precipitates can be utilised to enable the co-encapsulation and co-release of one hydrophilic and one hydrophobic model active from within a sole o/w emulsion microstructure. Co-release of the hydrophilic active entrapped within the biopolymer complexes is triggered by changes to the pH environment of the emulsion in a similar manner to the behaviour seen when release is taking place in aqueous dispersions of the NaCAS/CS co-precipitates alone. Discharge of the active is shown to be via relaxation and occurs as a result of swelling of the complexes, which is promoted by the pH-driven weakening of the electrostatic (attractive) forces between their protein and polysaccharide components. On the other hand, co-release of the hydrophobic active contained within the oil droplets of the emulsion is not affected by changes to pH conditions and instead is primarily controlled by the passage of the active through the interfacial barrier that exists at the droplet surface. Therefore, the present proof-of-principle study offers evidence that the employed microstructural approach can be utilised for the segregated co-encapsulation and independent co-release of two incompatible actives, thus proposing an alternative route for the development of novel emulsion-based liquid formulations containing multiple actives, with direct applications in the agrochemical, pharmaceutical, personal care and foods sectors.

## AUTHOR INFORMATION


### Corresponding Author

*F.Spyropoulos@bham.ac.uk


### Author Contributions

The manuscript was written through contributions of all authors. All authors have given approval to the final version of the manuscript.


### Funding Sources

The authors would also like to thank the Engineering and Physical Research Council (EPSRC), Innovate UK and Syngenta for provision of funding to carry out the work presented here.

## ACKNOWLEDGMENT

The authors are grateful to Dr Robin Hancocks for his valuable assistance in confocal microscopy.


## ABBREVIATIONS

NaCAS, sodium caseinate; CS, chitosan; FSS, fluorescein sodium salt; RhodB, rhodamine B; DMP, dimethylphthalate; PE, perylene; UV-VIS, ultraviolet-visible; SFO, sunflower oil.

## REFERENCES


(1) Wang, H. - C.; Zhang, Y.; Possanza, C. M.; Zimmerman, S. C.; Cheng, J.; Moore, J. S.; Harris, K.; Katz, J. S. Trigger chemistries for better industrial formulations. *ACS Appl. Mater. Interfaces* **2015**, *7(12)*, 6369-6382.

(2) Drusch, S.; Mannino, S. Patent-based review on industrial approaches for the microencapsulation of oils rich in polyunsaturated fatty acids. *Trends Food Sci. Technol.* **2009**, *20(6-7)*, 237-244.

(3) Wu, F.; Jin, T. Polymer-based sustained-release dosage forms for protein drugs, challenges, and recent advances. *AAPS PharmSciTech* **2008**, *9(4)*, 1218-1229.

(4) Windbergs, M.; Zhao, Y.; Heyman, J.; Weitz, D. A. Biodegradable core-shell carriers for simultaneous encapsulation of synergistic actives. *J. Am. Chem. Soc.* **2013**, *131*, 7933−7937.

(5) 05 Aditya, N. P.; Aditya, S.; Yang, H.; Kim, H. W.; Park, S. O.; Ko, S. Co-delivery of hydrophobic curcumin and hydrophilic catechin by a water-in-oil-in-water double emulsion. *Food Chem.* **2015**, *173*, 7-13.

(6) Čejková, J.; Štěpánek, F. Compartmentalized and internally structured particles for drug delivery - A review. *Curr. Pharm. Des.* **2013**, *19(35)*, 6298-6314.

(7) Li, N.; Zhao, L.; Qi, L.; Li, Z.; Luan, Y. Polymer assembly: Promising carriers as co-delivery systems for cancer therapy. *Prog. Polym. Sci.* **2016**, *58*, 1-26.

(8) Khaled, S. A.; Burley, J. C.; Alexander, M. R.; Yang, J.; Roberts, C. J. 3D printing of tablets containing multiple drugs with defined release profiles. *Int. J. Pharm.* **2015**, *494*, 643-650.

(9) Ma, L.; Kohli, M.; Smith, A. Nanoparticles for combination drug therapy. *ACS Nano* **2013**, *7(11)*, 9518-9525.

(10) Norton, J. E.; Gonzalez Espinosa, Y.; Watson, R. L.; Spyropoulos, F.; Norton, I. T. Functional food microstructures for macronutrient release and delivery. *Food Funct.* **2015**, *6(3)*, 663-678.

(11) Garrec, D. A.; Frasch-Melnik, S.; Henry, J. V. L.; Spyropoulos, F.; Norton, I. T. Designing colloidal structures for micro and macro nutrient content and release in foods. *Faraday Discuss.* **2012**, *158*, 37-49.

(12) Leng, D. E.; Calabrese, R. V. Immiscible Liquid–Liquid Systems. In *Handbook of Industrial Mixing: Science and Practice*; Paul, E. L., Atiemo-Obeng, V. A., Kresta, S. M., Eds.; John Wiley & Sons, Inc.: New Jersey, 2004; Vol. 1, pp 639-753.

(13) Callender, S. P.; Mathews, J. A.; Kobernyk, K.; Wettig, S. D. Microemulsion utility in pharmaceuticals: Implications for multi-drug delivery. *Int. J. Pharm.* **2017**, *526(1-2)*, 425-442.

(14) Chong, D. T.; Liu, X. S.; Ma, H. J.; Huang, G. Y.; Han, Y. L.; Cui, X. Y.; Yan, J. J.; Xu, F. Advances in fabricating double-emulsion droplets and their biomedical applications. *Microfluid Nanofluidics* **2015**, *19(5)*, 1071-1090.

(15) Peres, L. B.; Peres, L. B.; de Araújo, P. H. H.; Sayer, C. Solid lipid nanoparticles for encapsulation of hydrophilic drugs by an organic solvent free double emulsion technique. *Colloids Surf. B* **2016**, *140*, 317-323.

(16) Di Martino, A.; Pavelkova, A.; Maciulyte, S.; Budriene, S.; Sedlarik, V. Polysaccharide-based nanocomplexes for co-encapsulation and controlled release of 5-Fluorouracil and Temozolomide. *Eur. J. Pharm. Sci.* **2016**, *92*, 276-286.

(17) Cosco, D.; Paolino, D.; Maiuolo, J.; Di Marzio, L.; Carafa, M.; Ventura, C. A.; Fresta, M. Ultradeformable liposomes as multidrug carrier of resveratrol and 5-fluorouracil for their topical delivery. *Int. J. Pharm.* **2015**, *489(1-2)*, 1-10.

(18) Ingebrigtsen, S. G.; Škalko-Basnet, N.; Jacobsen, C. de A. C.; Holsæter, A. M. Successful co-encapsulation of benzoyl peroxide and chloramphenicol in liposomes by a novel manufacturing method - dual asymmetric centrifugation. *Eur. J. Pharm. Sci.* **2017**, *97*, 192-199.

(19) Sharma, V.; Anandhakumar, S.; Sasidharan, M. Self-degrading niosomes for encapsulation of hydrophilic and hydrophobic drugs: An efficient carrier for cancer multi-drug delivery. *Mater. Sci. Eng. C* **2015**, *56*, 393-400.

(20) Vladisavljević, G. T. Recent advances in the production of controllable multiple emulsions using microfabricated devices. *Particuology* **2016**, *24*, 1-17.

(21) Choi, C.-H.; Weitz, D. A.; Lee, C.-S. One step formation of controllable complex emulsions: from functional particles to simultaneous encapsulation of hydrophilic and hydrophobic agents into desired position. *Adv. Mater.* **2013**, *25*, 2536-2541.

(22) Lai, W. F.; Susha, A. S.; Rogach, A. L. Multicompartment microgel beads for co-delivery of multiple drugs at individual release rates. *ACS Appl. Mater. Interfaces* **2016**, *8(1)*, 871-880.

(23) Lai, W. F.; Lin, M. C. Chemotherapeutic Drugs Interfere with Gene Delivery Mediated by Chitosan-Graft-Poly(Ethylenimine). *PLoS One* **2015**, *10(5)*, e0126367.

(24) Baillot, M.; Bentaleb, A.; Laurichesse, E.; Schmitt, V.; Backov, R. Triggering the mechanical release of mineralized Pickering emulsion-based capsules. *Langmuir* **2016**, *32(16)*, 3880-3889.

(25) Tadros, T. F. Controlled-release formulations. In *Colloids in Agrochemicals;* Colloids and Interface Science Series 5; WILEY-VCH: Weinheim, 2009 pp 235-246.

(26) Manojlović, V.; Nedović, V. A.; Kailasapathy, K.; Zuidam, N. J. Encapsulation of Probiotics for use in Food Products. In *Encapsulation Technologies for Active Food Ingredients and Food Processing*; Zuidam, N.J., Nedovic, V. Eds.; Springer: New York, 2010; pp 269-302.

(27) Vignati, E.; Piazza, R.; Lockhart, T. P. Pickering emulsions: Interfacial tension, colloidal layer morphology, and trapped-particle motion. *Langmuir* **2003**, *19(17)*, 6650-6656.

(28) Stancik, E. J.; Kouhkan, M.; Fuller, G. G. Coalescence of particle-laden fluid interfaces. *Langmuir* **2004**, *20(1)*, 90-94.

(29) Ashby, N. B.; Binks, B. P. *Phys.* Pickering emulsions stabilised by Laponite clay particles. *Phys. Chem. Chem. Phys.* **2000**, *2*, 5640-5646.

(30) Frelichowska, J.; Bolzinger, M.-A.; Chevalier, Y. Pickering emulsions with bare silica. *Colloids Surf. A* **2009**, *343*, 70-74.

(31) Pawlik, A.; Kurukji, D.; Norton, I. T.; Spyropoulos, F. Food-grade Pickering emulsions stabilised with solid lipid particles. *Food Funct.* **2016**, *7*, 2712-2721.

(32) Duffus, L.J.; Norton, J.E.; Smith, P.; Norton, I.T.; Spyropoulos, F. A comparative study on the capacity of a range of food-grade particles to form stable O/W and W/O Pickering emulsions. *J. Colloid Interface Sci.* **2016**, *473*, 9-21.

(33) Dickinson, E. Use of nanoparticles and microparticles in the formation and stabilization of food emulsions. *Trends Food Sci. Technol.* **2012**, *24*, 4-12.

(34) Walther, A.; Müller, A. H. E. Janus particles. *Soft Matter* **2008**, *4*, 663-668.

(35) Du, J.; O'Reilly, R. K. Anisotropic particles with patchy, multicompartment and Janus architectures: preparation and application. *Chem. Soc. Rev.* **2011**, *40*, 2402-2416.

(36) Binks, B. P.; Fletcher, P. D. I. Particles adsorbed at the oil−water interface: A theoretical comparison between spheres of uniform wettability and "Janus" particles. *Langmuir* **2001**, *17*, 4708-4710.

(37) Hong, L.; Jiang, S.; Granick, S. Simple method to produce Janus colloidal particles in large quantity. *Langmuir* **2006**, *22*, 9495-9499.

(38) Miller, R.; Fainerman, V. B.; Kovalchuk, V. I.; Grigoriev, D. O.; Leser, M. E.; Michel, M. Composite interfacial layers containing micro-size and nano-size particles. *Adv. Colloid Interface Sci.* **2006**, *128-130*, 17-26.

(39) Berton-Carabin, C. C.; Schroën, K. Pickering emulsions for food applications: Background, trends, and challenges. *Annu. Rev. Food Sci. Technol.* **2015**, *6*, 263-297.

(40) Binks, B. P.; Lumsdon, S. O. Influence of particle wettability on the type and stability of surfactant-free emulsions. *Langmuir* **2000**, *16*, 8622-8631.

(41) Shah, B.R.; Li, Y.; Jin, W.; An, Y.; He, L.; Li, Z.; Xu, W.; Li, B. Preparation and optimization of Pickering emulsion stabilized by chitosan-tripolyphosphate nanoparticles for curcumin encapsulation. *Food Hydrocoll.* **2016**, *52*, 369-377.

(42) Simovic, S.; Ghouchi-Eskandar, N.; Prestidge, C.A. Pickering emulsions for dermal delivery. *J. Drug Delivery Sci. Technol.* **2011**, *21(1)*, 123-133.

(43) Tambuwala, M. M.; Manresa, M. C.; Cummins, E. P.; Aversa, V.; Coulter, I. S.; Taylor, C. T. Targeted delivery of the hydroxylase inhibitor DMOG provides enhanced efficacy with reduced systemic exposure in a murine model of colitis. *J. Control. Release* **2015**, *217*, 221-227.

(44) Elzoghby, O.; El-Fotoh, W. S.; Elgindy, N. A. Casein-based formulations as promising controlled release drug delivery systems. *J. Control. Release* **2011**, *153*, 206-216.

(45) Ravi Kumar, M. N. V.; Muzzarelli, R. A. A.; Muzzarelli, C.; Sashiwa, H.; Domb, A. J. Chitosan Chemistry and Pharmaceutical Perspectives. *Chem. Rev.* **2004**, *104*, 6017-6084.

(46) Baldrick, P. The safety of chitosan as pharmaceutical excipient. *Regul. Toxicol. Pharmacol.* **2010**, *56*, 290-299.

(47) Bouyer, E.; Mekhloufi, G.; Rosilio, V.; Grossiord, J. - L.; Agnely, F. Proteins, polysaccharides, and their complexes used as stabilizers for emulsions: Alternatives to synthetic surfactants in the pharmaceutical field? *Int. J. Pharm.* **2012**, *436(1-2)*, 359-378.

(48) Kurukji, D.; Norton, I. T.; Spyropoulos, F. Fabrication of sub-micron protein-chitosan electrostatic complexes for encapsulation and pH-Modulated delivery of model hydrophilic active compounds. *Food Hydrocoll.* **2016**, *53*, 249-260.

(49) Amara, C.B.; Eghbal, N.; Degraeve, P.; Gharsallaoui, A. Using complex coacervation for lysozyme encapsulation by spray-drying. *J. Food Eng.* **2016**, *183*, 50-57.

(50) Turgeon, S. L.; Schmitt, C.; Sanchez C. Protein–polysaccharide complexes and coacervates. *Curr. Opin. Colloid Interface Sci.* **2007**, *12*, 166-178.

(51) Dickinson, E. Interfacial structure and stability of food emulsions as affected by protein-polysaccharide interactions. *Soft Matter* **2008**, *4(5)*, 932-942.

(52) Evans, M.; Ratcliffe, I.; Williams, P.A. Emulsion stabilisation using polysaccharide–protein complexes. *Curr. Opin. Colloid Interface Sci.* **2013**, *18(4)*, 272-282.

(53) Dickinson, E.; Semenova, M. G. Emulsifying properties of covalent protein-dextran hybrids. *Colloids Surf.* **1992**, *64(3)*, 299-310.

(54) Jourdain, L.; Leser, M. E.; Schmitt, C.; Michel, M.; Dickinson, E. Stability of emulsions containing sodium caseinate and dextran sulfate: Relationship to complexation in solution. *Food Hydrocoll.* **2008**, *22(4)*, 647-659.

(55) Semenova, M. Protein–polysaccharide associative interactions in the design of tailor-made colloidal particles. *Curr. Opin. Colloid Interface Sci.* **2017**, *28*, 15-21.

(56) Wang, L. J.; Hu, Y. Q.; Yin, S. W.; Yang, X. Q.; Lai, F. R.; Wang, S. Q. Fabrication and characterization of antioxidant pickering emulsions stabilized by zein/chitosan complex particles (ZCPs). *J. Agric. Food Chem.* **2015**, *63*, 2514-2524.

(57) Wang, X.; Wang, Y.; Wei, K.; Zhao, N.; Zhang, S.; Chen, J. Drug distribution within poly(ε-caprolactone) microspheres and in vitro release. *J. Mater. Process. Technol.* **2009**, *209(1)*, 348-354.

(58) Howard, P. H.; Banerjee, S; Robillard, K. H. Measurement of water solubilities, octanol/water partition coefficients and vapor pressures of commercial phthalate esters. *Environ. Toxicol. Chem.* **1985**, *4(5)*, 653-661.

(59) Ritger, P. L.; Peppas, N. A. A simple equation for description of solute release II. Fickian and anomalous release from swellable devices. *J. Control. Release* **1987**, *5(1)*, 37-42.

(60) Peppas, N. A.; Sahlin. J. J. A simple equation for the description of solute release. III. Coupling of diffusion and relaxation. *Int. J. Pharm.* **1989**, *57(2)*, 169-172.

(61) Guy, R. H.; Hadgraft, J.; Kellaway, I. W.; Taylor, M. J. Calculations of drug release rates from particles. *Int. J. Pharm.* **1982**, *11(3)*, 199-207.

(62) Washington, C.; Evans, K. Release rate measurements of model hydrophobic solutes from submicron triglyceride emulsions. *J. Control. Release* **1995**, *33(3)*, 383-390.

(63) Schmitt, C.; Turgeon, S.L. Protein/polysaccharide complexes and coacervates in food systems. *Adv. Colloid Interface Sci*. **2011**, *167(1)*, 63-70.

(64) de Kruif, C. G.; Weinbreck, F.; de Vries, R. Complex coacervation of proteins and anionic polysaccharides. *Curr. Opin. Colloid Interface Sci.* **2004**, *9(5)*, 340-349.

(65) Picone, C. S. F.; Cunha, R. L. Chitosan–gellan electrostatic complexes: Influence of preparation conditions and surfactant presence. *Carbohydr. Polym.* **2013**, *94(1)*, 695-703.

(66) O'Kennedy, B. T. Caseins. In *Handbook of Food Proteins*; Phillips, G. O., Williams, P. A., Eds.; Woodhead Publishing: Cambridge, 2011; pp 13-29.

(67) Xu, P.; Bajaj, G.; Shugg T.; Van Alstine, W. G.; Yeo, Y. Zwitterionic chitosan derivatives for pH-sensitive stealth coating. *Biomacromolecules* **2010**, *11(9)*, 2352-2358.

(68) Qun, G.; Ajun, W. Effects of molecular weight, degree of acetylation and ionic strength on surface tension of chitosan in dilute solution. *Carbohydr. Polym.* **2006**, *64(1)*, 29-36.

(69) Atkinson, P. J.; Dickinson, E.; Horne, D. S.; Richardson, R. M. Neutron reflectivity of adsorbed *β*-casein and *β*-lactoglobulin at the air/water interface. *J. Chem. Soc. Faraday Trans.* **1995**, *91(17)*, 2847-2854.

(70) Harnsilawat, T.; Pongsawatmanit, R.; McClements, D. J. Characterization of β-lactoglobulin–sodium alginate interactions in aqueous solutions: A calorimetry, light scattering, electrophoretic mobility and solubility study. *Food Hydrocoll.* **2006**, *20(5)*, 577-585.

(71) Santoro, M.; Marchetti, P.; Rossi, F.; Perale, G.; Castiglione, F.; Mele, A.; Masi, M. Smart approach to evaluate drug diffusivity in injectable agar-carbomer hydrogels for drug delivery. *J. Phys. Chem. B* **2011**, *115(11)*, 2503-2510.

(72) Mauri, E.; Chincarini, G. M. F.; Rigamonti, R.; Magagnin, L.; Sacchetti, A.; Rossi, F. Modulation of electrostatic interactions to improve controlled drug delivery from nanogels. *Mater. Sci. Eng. C* **2017**, *72*, 308-315.

(73) Piyakulawat, P.; Praphairaksit, N.; Chantarasiri, N.; Muangsinet, N. Preparation and evaluation of chitosan/carrageenan beads for controlled release of sodium diclofenac. *AAPS PharmSciTech* **2007**, *8(4)*, 120.

(74) Jones, O. G.; McClements, D. J. Functional biopolymer particles: Design, fabrication, and applications. *Compr. Rev. Food Sci. Food Saf.* **2010**, *9*, 374-397.

(75) Perrechil, F. A.; Cunha, R. L. Oil-in-water emulsions stabilized by sodium caseinate: Influence of pH, high-pressure homogenization and locust bean gum addition. *J. Food Eng.* **2010**, *97(4)*, 441-448.

(76) Nilsen-Nygaard, J.; Strand, S.P.; Vårum, K.M.; Draget, K.I.; Nordgård, C.T. Chitosan: Gels and interfacial properties. *Polymers* **2015**, *7*, 552-579.

(77) Payet, L.; Terentjev, E. M. Emulsification and stabilization mechanisms of O/W emulsions in the presence of chitosan. *Langmuir* **2008**, *24*, 12247–12252.

(78) Semenova, M. G.; Belyakova, L. E.; Polikarpov, Y. N.; Antipova, A. S.; Dickinson, E. Light scattering study of sodium caseinate+dextran sulfate in aqueous solution: Relationship to emulsion stability. *Food Hydrocoll.* **2009**, *23(3)*, 629-639.

(79) Nakatani, K.; Miyanaga, M.; Kawasaki, Y. Mass transfer of water-insoluble organic compound from octadecylsilyl-silica gel into water in the presence of a nonionic surfactant. *Anal. Sci.* **2011**, *27(12)*, 1253-1256.

(80) Howard, S. C.; Craig, V. S. J.; FitzGerald, P. A.; Wanless, E. J. Swelling and collapse of an adsorbed pH-responsive film-forming microgel measured by optical reflectometry and QCM. *Langmuir* **2010**, *26(18)*, 14615-14623.

(81) Trotta, M. Influence of phase transformation on indomethacin release from microemulsions. *J. Control. Release* **1999**, *60(2-3)*, 399-405.